Ultrafast 2D NMR: An Emerging Tool in Analytical Spectroscopy

Patrick Giraudeau[1] and Lucio Frydman[2]

[1]Chimie et Interdisciplinarité: Synthèse, Analyse, Modélisation, UMR 6230, Université de Nantes, 44322 Nantes Cedex 03, France; email: patrick.giraudeau@univ-nantes.fr

[2]Department of Chemical Physics, Weizmann Institute of Science, 76100 Rehovot, Israel; email: lucio.frydman@weizmann.ac.il

Annu. Rev. Anal. Chem. 2014. 7:129–61

The *Annual Review of Analytical Chemistry* is online at anchem.annualreviews.org

This article's doi:
10.1146/annurev-anchem-071213-020208

Keywords

NMR spectroscopy, 2D NMR, ultrafast NMR, spatiotemporal encoding, real-time NMR, quantitative analysis

Abstract

Two-dimensional nuclear magnetic resonance (2D NMR) spectroscopy is widely used in chemical and biochemical analyses. Multidimensional NMR is also witnessing increased use in quantitative and metabolic screening applications. Conventional 2D NMR experiments, however, are affected by inherently long acquisition durations, arising from their need to sample the frequencies involved along their indirect domains in an incremented, scan-by-scan nature. A decade ago, a so-called ultrafast (UF) approach was proposed, capable of delivering arbitrary 2D NMR spectra involving any kind of homo- or heteronuclear correlation, in a single scan. During the intervening years, the performance of this subsecond 2D NMR methodology has been greatly improved, and UF 2D NMR is rapidly becoming a powerful analytical tool experiencing an expanded scope of applications. This review summarizes the principles and main developments that have contributed to the success of this approach and focuses on applications that have been recently demonstrated in various areas of analytical chemistry—from the real-time monitoring of chemical and biochemical processes, to extensions in hyphenated techniques and in quantitative applications.

1. INTRODUCTION

NMR: nuclear magnetic resonance

Fourier transform (FT): a mathematical procedure enabling the distinguishing of frequency contributions that compose time-dependent signal response functions

Nuclear magnetic resonance (NMR) is a highly versatile spectroscopic technique with applications in a large range of disciplines, from chemistry and physics to biology and medicine. It is widely used as an analytical tool in all chemistry laboratories and industries, where it provides a superior way to extract structural and quantitative information on the site-resolved level and hence enables the unambiguous elucidation of inorganic and organic molecular structures (1, 2). Common NMR isotopes include ^{1}H, ^{13}C, ^{15}N, ^{19}F, ^{31}P, and many others. NMR is also very well recognized in biochemistry for its ability to deliver the folding and geometry of large macromolecules, alone or in complexes with drugs or with other biomacromolecules, under nearly physiological conditions (3, 4). The capabilities of NMR to shed light on dynamic chemical, biophysical, and biological processes over a wide range of timescales by a range of complementary methods are also well known (5). Enabling many—in fact most—of these applications was a revolutionary proposition by J. Jeener, dating back to 1971 and involving the concept of multidimensional NMR spectroscopy acquisitions (6). By providing a way of spreading the spectral peaks over a 2D frequency plane rather than along a 1D frequency axis, Jeener's idea literally changed the face of magnetic resonance as it offered (*a*) a much better way of discriminating resonances than what could be offered by 1D traces—even at much higher fields—and (*b*) a much richer and wider range of experiments for extracting structural and dynamic information maps, of a kind that is impossible for other spectroscopic methods relying on 1D acquisitions (6, 7). As a result, 2D NMR, as well as its higher-dimensional variants, has now become a routine analytical tool for the elucidation of small organic molecules and a method of choice for the study of solution- and solid-state macromolecular structures. Readers are referred to the literature for tutorials on these aspects (8).

The ingenuity of the 2D NMR concept consists in reconstructing a correlation between two interconnected spin evolution frequencies, using a series of statistically independent 1D NMR acquisitions. Indeed, in conventional Fourier (pulsed) NMR, 1D spectra are obtained by exciting spins with an appropriate pulse sequence and then monitoring their evolution in real time. As spins precess, they will emit a signal that is inductively picked up; Fourier analysis of this signal as a function of the acquisition time t will reveal the intervening spin evolution frequencies. 2D NMR will eventually deliver a bidimensional frequency correlation by incrementing two evolution times rather than just one. Although physically speaking there are no two time variables, 2D NMR overcomes this obstacle by performing a series of 1D experiments with one particular delay in the sequence—the so-called indirect-domain time variable—incremented in constant steps from scan to scan. When considering the acquisition of the ensuing spin signal as a function of the physical evolution time, also referred to as the direct domain, one arrives at the canonical sequence of events generalized by Ernst and coworkers' (7, 10, 11) landmark papers in this field:

$$\text{preparation} - \text{evolution}\ (t_1) - \text{mixing} - \text{detection}\ (t_2). \qquad 1.$$

Here the preparation and the mixing events denote sequences that remain constant throughout the series of intervening scans. The repetition of this series with incremented values of t_1 leads, after collecting each of the resulting data sets as a function of the conventional acquisition time t_2, to a 2D signal $S(t_1, t_2)$, depending on the two time variables. This complex matrix can be viewed as a 2D extension of a normal free induction decay (FID); a Fourier transform (FT) of this FID—this time in a generalized time-domain plane—gives rise to a 2D spectrum $S(\Omega_1, \Omega_2)$. The frequencies (Ω_1, Ω_2) involved along the axes of this spectrum depend on the spin evolution that has taken place during the t_1, t_2 periods, as well as on the preparation and mixing sequences that preceded them.

In principle, the scheme in Equation 1 is extremely general, and various experiments are based on it. In chemical and biophysical applications, they are usually used to correlate the chemical

shifts of two identical or two different nuclear species. This gives rise to families of so-called homo- or heteronuclear 2D correlation experiments, with correlation spectroscopy (COSY) (7) and nuclear Overhauser effect spectroscopy (12) as main members of the former, and heteronuclear single-quantum correlation (HSQC) (13), heteronuclear multiple-quantum correlation (HMQC) (14), and heteronuclear multiple-bond correlation (HMBC) (15) as main members of the latter. The idea of 2D NMR can also be used to separate two interactions acting on the same spin; this is the case in J-res spectroscopy, which correlates homo- or heteronuclear J-couplings along one axis, with chemical shift evolution along the second. Even within the context of single-spin interactions, the ideas of Ernst and coworkers (7, 16–18) are very powerful, and they underlie the field of 2D magnetic resonance imaging (MRI), where the evolution of spins (usually water ^{1}Hs) is monitored under the action of consecutive magnetic field gradients applied along orthogonal directions, to enable the noninvasive characterization of opaque objects containing ^{1}H, ^{31}P, or ^{19}F. The success and power of 2D spectroscopy is an essential ingredient of most uses of NMR. This popularity is reflected by its ubiquitous presence in complex molecular analyses, its use in correlating information (chemical shifts, couplings, etc.) between different nuclei, and exploitation in dynamic studies. 2D NMR provides, in sum, an incredibly helpful tool in organic (19, 20) and analytical chemistry (21, 22), as well as in structural biology (23, 24), pharmaceutical analyses (25), and ultimately in clinical diagnostics.

In spite of its uniquely wide range of applications, 2D NMR suffers from an intrinsic drawback vis-à-vis its 1D counterpart. Due to the numerous t_1 increments (typically several hundred) needed to sample the indirect dimension with sufficient spectral width and resolution, long experimental durations are a built-in feature of these experiments—regardless of sensitivity considerations. Long experimental durations have several consequences. Some of them are practical such as the loading of a spectrometer schedule that may translate into significant costs. A more fundamental consequence is the inability to study samples in which composition evolves within the timescale of the 2D experiment. This is the case not only for samples undergoing chemical reactions or dynamic processes, but also for chemical and biological samples with limited lifetimes. Another important repercussion of the experimental duration is that long experiments are more likely to be affected by spectrometer instabilities over time (26, 27). This will generate additional noise in the indirect dimension, due to the long time interval (several seconds) between the acquisition of two successive points of the pseudo-FID, thus affecting the analytical performance of 2D NMR experiments. Another important class of experiments incompatible with conventional 2D acquisition schemes comprises experiments on metastable states—foremost among them are experiments relying on hyperpolarized spin states seeking rapid decay back to thermal (Boltzmann) equilibrium.

During recent years, numerous strategies have been proposed for reducing the duration of 2D NMR experiments. The first family of approaches consists of optimizing conventional pulse sequences to reduce the recovery delay separating two successive t_1 increments. This can be performed by a careful optimization of pulse angles and delays (28, 29), the addition of paramagnetic relaxation agents (30), or implementation of gradient-based fast-repetition crushing (i.e., coherence selection) schemes (31). All of these strategies can lead to a dramatic reduction of the recovery delay in 2D NMR experiments; particularly impressive gains have resulted when implementing optimized excitations in large cross-relaxing biomolecules. Another series of complementary approaches seek to reduce the constraints of Nyquist sampling criteria; their aim is to explore the components involved in the indirect-domain evolution with no compromises on the width or resolution of the resulting spectra—but without having to abide by Nyquist's stringent demands. These efforts usually involve departing from the fast FT and relying instead on alternative forms of Fourier analysis. These involve unfolding approaches based on optimized dealiazing procedures (32). They also involve compressed sensing approaches that reduce the experimental

Correlation spectroscopy (COSY): a common type of homonuclear 2D experiment showing connectivities between scalarly coupled spins

Nuclear Overhauser effect spectroscopy: a homonuclear 2D experiment showing connectivities between spins depending on their spatial proximity

Heteronuclear single-quantum correlation (HSQC): a common heteronuclear 2D experiment for determining connectivities between heteronuclear pairs (e.g., ^{1}H and ^{13}C) via a single quantum time evolution

Heteronuclear multiple-quantum correlation (HMQC): a common heteronuclear 2D experiment for determining connectivities between heteronuclear pairs (e.g., ^{1}H and ^{13}C) via a multiple-quantum time evolution

Heteronuclear multiple-bond correlation (HMBC): a common heteronuclear 2D experiment for determining long-distance coupling between heteronuclear pairs (e.g.,^{1} H and ^{13}C)

duration without sacrificing resolution with post-processing based on ℓ_1-norm minimization (33, 34), linear prediction (35, 36), maximum entropy reconstruction (36, 37), or numerical integration approaches (38) in which algorithms are applied to reconstruct a complete FID in the F_1 dimension from a limited number of points. However, covariance NMR methodologies (39), in which the covariance matrix of the experimental data is calculated, resulting in high-resolution improvement, are other alternatives. Many of these alternatives involve randomly sampling the (t_1, t_2) space to reduce the number of increments. Several strategies have been proposed, including exponential (40), radial (41), and random sampling (42). These approaches are often combined with one of the nonconventional processing methods described above (43). Hadamard spectroscopy provides yet another fast acquisition alternative worth highlighting, which, by relying on an excitation in the frequency domain, departs from the Fourier-based methodology (44) to deliver 2D spectra.

Most approaches described above aim at reducing the number of t_1 increments in the indirect dimension but are still based on the basic data sampling approach given in Equation 1. Thus, although all these strategies can accelerate the sampling of 2D NMR data, and although much faster than conventional 2D NMR acquisitions and very promising for various applications in NMR spectroscopy, all these methods will still require numerous scans associated with 10–100-s acquisition times to deliver their spectral correlations. In 2002, a different strategy centered on imaging principles was proposed, which provides an entirely new way of acquiring multidimensional spectra. This approach made possible for the first time the acquisition of arbitrary 2D NMR or MRI correlations—in liquids and solids, in vitro or in vivo—in a single scan. This led to the so-called ultrafast (UF) NMR methodology (45, 46), which makes it possible to record any kind of 2D NMR spectrum in a single scan and as such, in a fraction of a second. During the past 10 years, the analytical performance of this methodology has been greatly improved, and UF NMR evolved from a tool for method development to a powerful analytical tool. The potential and performance of UF 2D NMR are shown in **Figure 1**, which highlights the quality of the subsecond spectra that this approach offers. This review aims at emphasizing the analytical potential of UF 2D NMR for a variety of applications. First, the principles of this methodology are summarized, as

J-res spectroscopy: a common type of homonuclear 2D experiment separating chemical shift and coupling interactions in two orthogonal dimensions

MRI: magnetic resonance imaging

Linear prediction: a signal processing procedure that improves the resolution of NMR spectra by predicting the missing points in a temporal signal

Maximum entropy reconstruction: a signal processing procedure that improves the resolution of NMR spectra recorded with a limited number of points

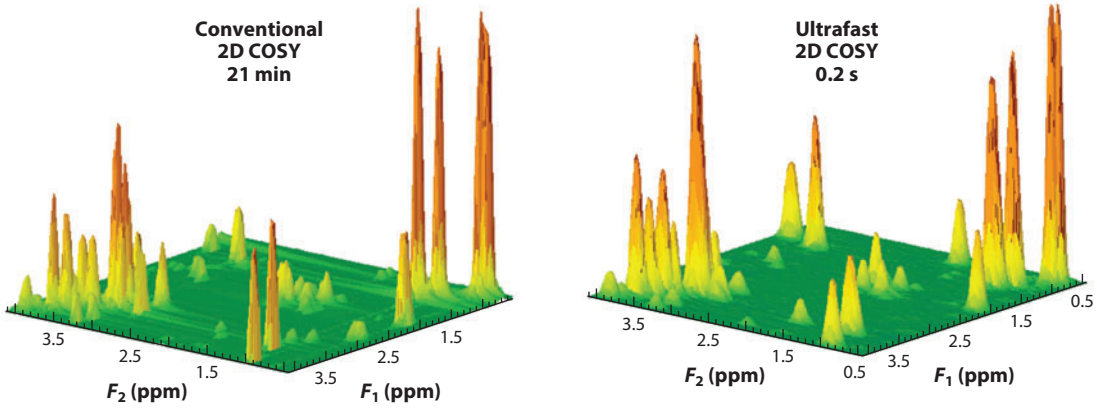

Figure 1

(*a*) Conventional and (*b*) UF 2D ^{1}H homonuclear spectra (COSY) recorded on a mixture of metabolites on a 500-MHz Avance III spectrometer equipped with a cryoprobe. Abbreviations: COSY, correlation spectroscopy; UF, ultrafast.

well as the developments that have increased its performance to make it a more nimble analytical tool. Then, applications and limitations of UF 2D NMR are illustrated in a variety of settings in which the experiment duration plays a crucial role: (*a*) the real-time study of samples whose composition evolves over time, where fast acquisition techniques are indispensable; (*b*) the field of quantitative analysis, where UF 2D NMR provides an original way to reach high precision for the high-throughput, quantitative analysis of complex mixtures; and (*c*) the coupling of UF 2D NMR with hyphenated and hyperpolarization techniques, where the single-scan nature offers a powerful solution to the irreversibility issue of the separation/preparation processes. Finally, we discuss the perspectives and challenges offered by this new analytical tool.

Hadamard spectroscopy: an alternative way of recording multidimensional NMR spectra in a non-Fourier fashion

2. PRINCIPLES OF UF 2D NMR

2.1. Basic Concepts

The UF methodology relies on the concept of imparting a spatiotemporal encoding of the spin interactions to be measured (45). The basic scheme of how this is implemented and how it can be put to use for the sake of monitoring the indirect-domain evolution frequencies in a single scan is summarized in **Figure 2**. It bases its description of the UF acquisition strategy on the Jeener-Ernst acquisition mode underlying conventional 2D NMR experiments and stresses how, instead of repeating N_1 successive experiments on the sample with an array of independent time

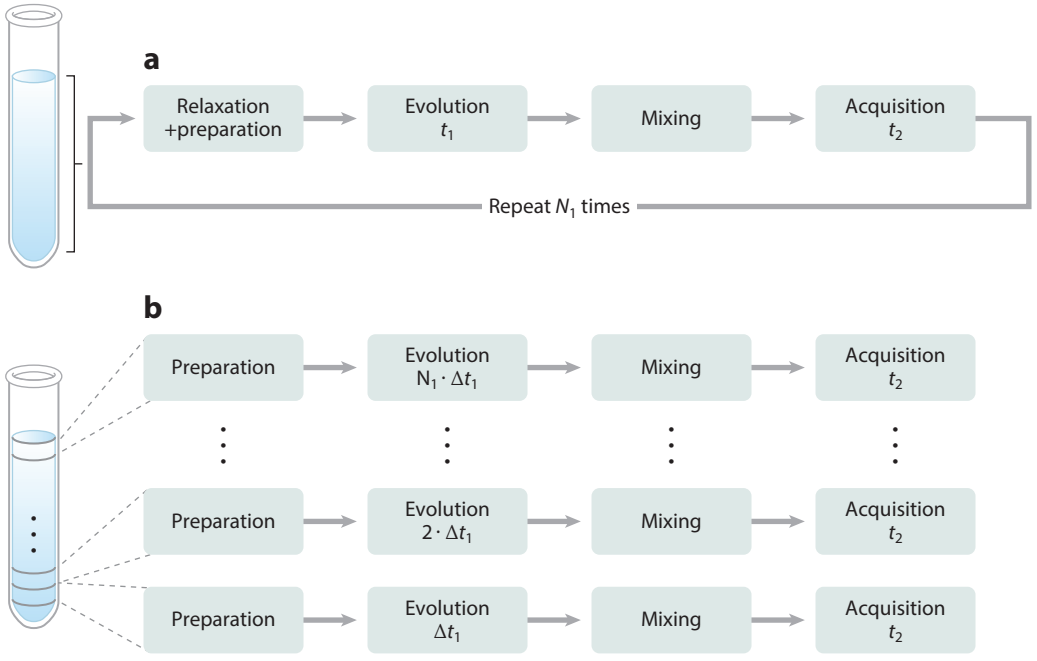

Figure 2

(*a*) Conventional versus (*b*) UF data acquisition schemes. (*a*) In conventional 2D NMR, N_1 experiments are repeated on the sample while incrementing the t_1 evolution period. A relaxation delay is necessary between each t_1 increment to let the magnetization return to its equilibrium position. (*b*) The UF 2D NMR experiment can be visualized as subdividing the sample into N_1 discrete slices (which may be of a nominal rather than of a real nature—the same argument would apply if the spatial evolution were continuously imposed) that simultaneously undergo different experiments with incremented t_1 delays. Abbreviations: NMR, nuclear magnetic resonance; UF, ultrafast.

increments (**Figure 2*a***), analogous information could result from dividing the sample into N_1 slices where the spins located at different positions undergo different evolution periods—but happening simultaneously for all slices within the course of the same scan (**Figure 2*b***). As in conventional 2D NMR, this spatiotemporal encoding period could be preceded by identical preparation periods for all slices and typically consisting of a relaxation delay followed by an excitation block. Also, like their conventional 2D counterparts, such spatiotemporal encoding will be followed by a mixing period that transfers coherences between indirect and direct domains. Finally, the signal is detected in a spatially specific fashion that allows one to distinguish the individual t_1 increments—for example, using an oscillating acquisition gradient such as the one characteristic of echo-planar spectroscopic imaging (EPSI) (47, 48). As such a scheme also enables one to monitor the post-mixing chemical shift evolution, an appropriate processing procedure enables one to extract the desired 2D spectrum from such a series of echo trains. And, although **Figure 2** makes a comparison between multiscan and single-scan acquisition modes based on a discrete partitioning of the spatial and temporal variables, the approach in **Figure 2*b*** is also amenable to a continuous encoding of the (analog) spatiotemporal variable.

Echo-planar spectroscopic imaging (EPSI): an acquisition technique that maps a spatial dimension and a spectroscopic dimension in a single readout

It follows that a key feature of the UF methodology is its requirement of creating an evolution period depending on the spatial location of the spins in the sample. This can be performed in numerous ways: in a discrete or continuous fashion, as well as in a real- or constant-time fashion. Original demonstrations included applying a series of frequency-selective pulses played out together with pairs of bipolar gradients along the z-axis (45, 46, 49); alternative modes include continuous spatiotemporal encoding schemes (50–56), where the sample can be considered as being divided into an infinite number of infinitesimal slices. All these schemes will provide, at the end of the spatiotemporal encoding period, a linear dephasing proportional to the position along the vertical z-axis. **Figure 3** illustrates how this can be achieved in a real-time (51) or constant-time (50) fashion. In all cases, a magnetic field gradient G_e is applied along the spatial axis, which causes the spins situated at different positions to undergo different resonance frequencies. If a chirp pulse (57, 58) with a linear frequency sweep is applied simultaneously, spins will be excited at a different time $t(z)$ according to their position z. The pulse/gradient combination described in **Figure 3*a*** is not sufficient to perform the spatiotemporal encoding step required by UF experiments, as it creates a quadratic z^2 dephasing that cannot be further refocused by linear gradients. Therefore, the first pulse is generally followed by a second suitable manipulation, for instance, an identical radio frequency (RF) pulse, but applied under the action of an opposite gradient. This scheme leads to a linear dephasing that is proportional to the position along the z-axis. This dephasing also depends on the resonance frequency Ω_1. In the real-time version proposed by Shrot and coworkers (51), this spatial encoding leads to an amplitude-modulated signal (**Figure 3*b***), whereas in the constant-time version proposed by Pelupessy (50), two 180° chirp pulses are applied following a nonselective 90° excitation pulse, resulting in a phase-modulated encoding (**Figure 3*c***). Several alternative schemes have been proposed for reaching a similar kind of linear dephasing (50–53, 55).

After achieving this site-specific linear dephasing, a mixing period is generally applied, allowing a transfer of information between scalar- or dipole-coupled spins, as is usual in conventional 2D NMR. This period is therefore identical to its conventional counterpart and will preserve the linear dephasing obtained after spatiotemporal encoding into the homo- or heteronuclear species that is going to be monitored during t_2. To refocus this dephasing and obtain an observable signal, a gradient G_a is applied while the receiver is open, leading to a series of site-specific spin-echoes whose timing matches in a one-to-one fashion the positions that represent the various sites' resonance frequencies (**Figure 4*a***). Because of the action of this gradient, a time-domain signal equivalent to the indirect domain's 1D spectrum is observed. No FT is needed to arrive

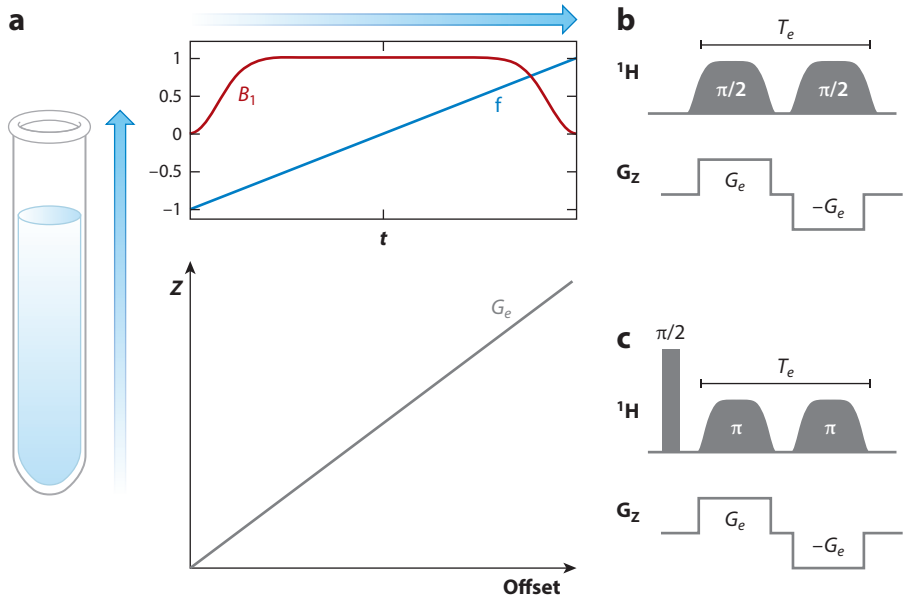

Figure 3

(*a*) Principle of continuous spatiotemporal encoding in UF 2D NMR. A chirp pulse with a linear frequency sweep is applied together with a magnetic field gradient G_e. As a result, spins located at different positions z are excited at different times $t(z)$. Pulse sequence elements proposed for performing continuous spatiotemporal encoding in a (*b*) real-time or (*c*) constant-time fashion. In both cases, two identical RF pulses are applied, sweeping between initial and final offsets $\pm\gamma_e G_e L/2$ at rates $2\pi R = \pm 2\gamma_e G_e L/T_e$ with amplitudes set so as to impart net $\pi/2$ or π rotations of the spins at all positions. The application of a first chirp pulse together with a gradient leads to a dephasing $\phi(z)$ containing a linear and a quadratic z-dependence. The latter is removed by the application of a second identical pulse applied with an opposite gradient, resulting in a linear dephasing $\phi(z)$ that also depends on the resonance frequency Ω_1. Abbreviations: NMR, nuclear magnetic resonance; RF, radio frequency; UF, ultrafast.

to this signal, which forms the first dimension of the 2D spectrum being sought. Because of this, the indirect domain is also referred to as the UF or the spatially encoded dimension, as it results from the spatiotemporal encoding process characterizing this method. Additionally, although this readout process can be made arbitrarily short by increasing G_a's strength, the resolution of the various site-specific echoes still demands sufficiently long spatiotemporal encoding periods—and therefore no Nyquist-derived criterion is actually broken by this readout process.

Under typical conditions, this gradient-driven readout of the indirect-domain information only lasts a few hundreds of microseconds—much less than the natural T_2 lifetimes of normal NMR signals. To obtain the second dimension of the 2D spectrum, a technique formally analogous to EPSI (47, 48) can be employed. In such an approach, the normal free evolution is replaced by an acquisition process incorporating a series of bipolar gradient pairs (**Figure 4*b***). These oscillating gradients lead to periodic refocusings and defocusings of the UF 1D "spectra"; a train of mirror-imaged echoes reflecting the direct-domain evolution of the 1D indirect-domain spectra thereby results. The system continues evolving during the course of this oscillating $\pm G_a$ train under the influence of conventional parameters (T_2 relaxation, direct-domain chemical shifts, J-couplings, etc.); the result of this additional evolution is akin to a 2D $S(F_1,t_2)$ interferogram—not unlike the one that would result from the 1D Fourier transformation of a conventional 2D NMR data set

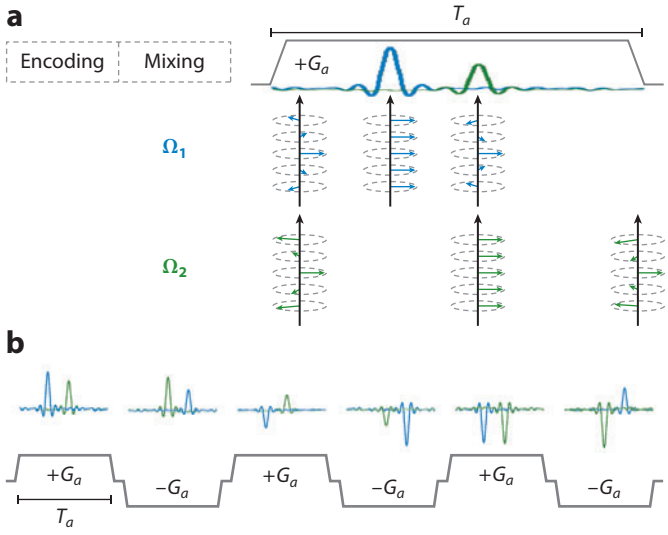

Figure 4

Signal detection in UF 2D NMR. (*a*) Acquisition of the ultrafast dimension. A magnetic field gradient of amplitude G_a and duration T_a is applied while the receiver is open, which refocuses the dephasing induced by spatiotemporal encoding. It leads to a series of echoes whose positions are proportional to resonance frequencies. (*b*) Acquisition of the conventional dimension. A series of subspectra are detected during a train of bipolar gradient pulses while the system evolves under the influence of conventional parameters (relaxation, chemical shifts, couplings, etc.). Data rearrangement and Fourier transform along the conventional dimension are necessary to obtain the final 2D spectrum. Abbreviations: NMR, nuclear magnetic resonance; UF, ultrafast.

against the indirect time-domain variable t_1. It follows that an appropriate data rearrangement followed by a conventional FT that discriminates the different resonance frequencies that were active over the course of the direct time domain t_2 can lead to the full information normally contained in a 2D NMR spectrum. As this second dimension arises from a conventional evolution, we refer to it as the direct domain. The overall procedure will therefore lead to the retrieval of a normal-looking 2D NMR spectrum—but collected within a single transient.

As a consequence of this particular data acquisition procedure, a specific type of processing is necessary to obtain the resulting 2D spectrum (45). This includes separating the mirror-image data acquired during positive and negative acquisition gradients to achieve constant Δt_2 increments for every F_1 coordinate, correcting for potential gradient offset by shearing the two resulting interferograms in the joint (F_1,t_2) domain, suitably weighting and Fourier transforming the resulting data along the direct domain, and adding, after inverting one of them along the F_1 dimension, the two resulting 2D spectra. The use of several homemade processing programs has been reported to perform this specific processing (45, 50, 56, 59, 60).

The UF methodology described above makes it possible to obtain in a single scan any kind of 2D NMR correlation, provided that the sensitivity is sufficient to deliver the information being sought in that one single scan. Apart from that, arbitrary UF pulse sequences can be designed to encode identical correlations or separations as their conventional counterpart, most often by morphing either constant- or real-time versions of the conventional sequences into spatiotemporally encoded counterparts and replacing their normal acquisition modules by suitably modulated EPSI acquisitions, incorporating homo- or heterodecoupling as per the sequence's needs. **Figure 5** presents representative examples of UF spectra obtained using commercial spectrometers,

together with the corresponding pulse sequences. Although not comprehensive, this figure is meant to illustrate the potential and versatility of this new analytical tool and to point out some of its characteristic features, such as resolution issues or its ability to incorporate standard phase cycling or sensitivity-enhancement issues associated with multiscan averaging (**Figure 5*d***).

2.2. UF 2D NMR: Features and Compromises

Despite its generality, UF 2D NMR is characterized by a specific sampling scheme and particular acquisition parameters, which give it a behavior that differs from its conventional counterparts. In particular, the gradients and chirp pulses involved in the initial encoding stage, as well as the EPSI-like detection scheme, may lead to numerous compromises. This will relate in particular to sensitivity, resolution, and spectral width issues (62–66) and can be summarized as follows below.

2.2.1. Spectral widths: Spectral widths SW^{UF} and SW^{Conv} in the UF and conventional dimensions, respectively, are related to the resolution in the UF dimension by the following equation (67):

$$\gamma_a G_a L = \frac{2 \cdot SW^{UF} \cdot SW^{Conv}}{\Delta\nu}, \qquad 2.$$

where $\Delta\nu$ is the peak width in the UF dimension, γ_a the gyromagnetic ratio of the detected nuclei, L the height of the detection coil, and G_a the amplitude of the acquisition gradients. This relation shows that increasing the spectral windows along any of the two dimensions without altering the targeted resolution will condition the gradient amplitude that is required by the experiment.

2.2.2. Resolution and sensitivity: As in conventional 2D NMR, the resolution along the direct, FT-based dimension will be determined by its acquisition duration. In UF NMR, this will in turn define the number of gradient pairs that need to be applied during the course of the acquisition. Typically, 100–200 gradient pair oscillations can be achieved with conventional hardware, assuming that each cycle lasts for ≈0.5 ms and that G_a does not exceed the amplitudes targeted for long pulses (≈10–15 G/cm for spectroscopy probes; approximately twice these values for diffusion-specific probes). This would result in 10–20 Hz linewidths along the direct domain; these are often acceptable values, which can be further increased by processing algorithms such as linear prediction. In such instances, the resolution of homo- and heteronuclear J-couplings is straightforward. Further resolution limiting factors, however, may arise in the spatially encoded dimension (cf. **Figure 5**). Some of the factors impacting resolution in this dimension are conventional, e.g., the duration of spatiotemporal encoding (63). Independently of the spatial-encoding scheme and in analogy with conventional time-domain spectroscopy, this duration will define the resolution of the indirect domain, which will be inversely proportional to the duration of spatiotemporal encoding $t_1^{max} = T_e$ (62). Consequently, resolution should be easy to increase simply by applying a

Figure 5

Examples of 2D spectra recorded in a single scan, shown together with the corresponding NMR pulse sequence. (*a*) Ultrafast constant-time J-resolved spectrum recorded in 500 ms at 500 MHz on a cinnamic acid sample in DMSO-d_6 (59). (*b*) Ultrafast constant-time COSY spectrum recorded in 100 ms at 500 MHz with a cryoprobe on a mixture of six metabolites (alanine, threonine, glutamic acid, valine, serine, myoinositol) in D_2O. (*c*) Ultrafast real-time TOCSY spectrum recorded in 150 ms at 500 MHz on an *n*-butylchloride sample in $CDCl_3$ (61). (*d*) Ultrafast real-time ^{1}H-^{13}C HSQC spectrum recorded in two scans at 800 MHz with a cryoprobe on a lyophilized protein A sample in D_2O (51). (*e*) Ultrafast constant-time ^{1}H-^{13}C HSQC spectrum recorded in a single scan following the injection of hyperpolarized vitamin E at a 12-mM concentration (61). Note that all signals may not be visible due to the choice of the contour levels. Abbreviations: COSY, correlation spectroscopy; DMSO, dimethyl sulfoxide; HSQC, heteronuclear single-quantum correlation; NMR, nuclear magnetic resonance; TOCSY, total correlation spectroscopy.

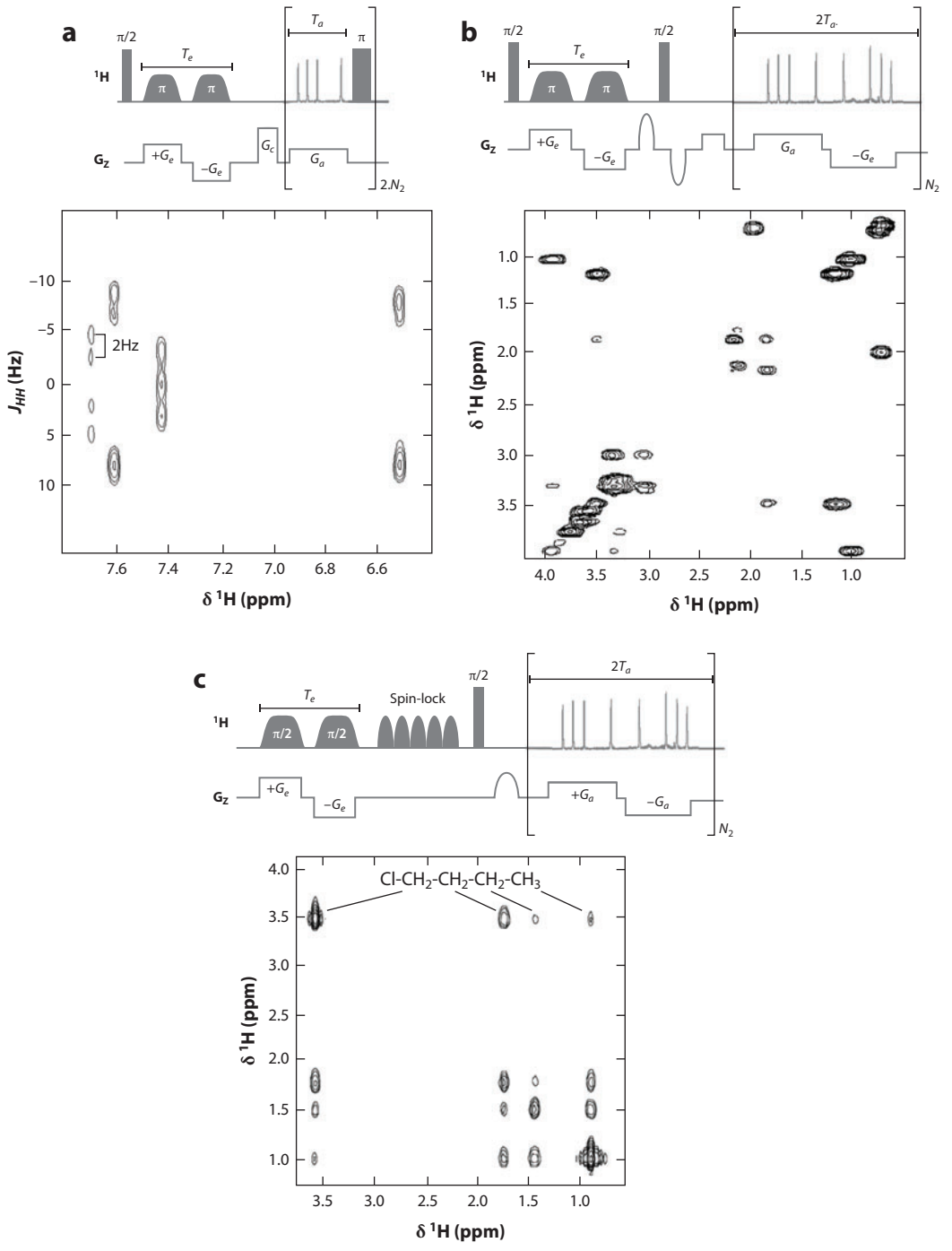

Figure 5

(*Continued*)

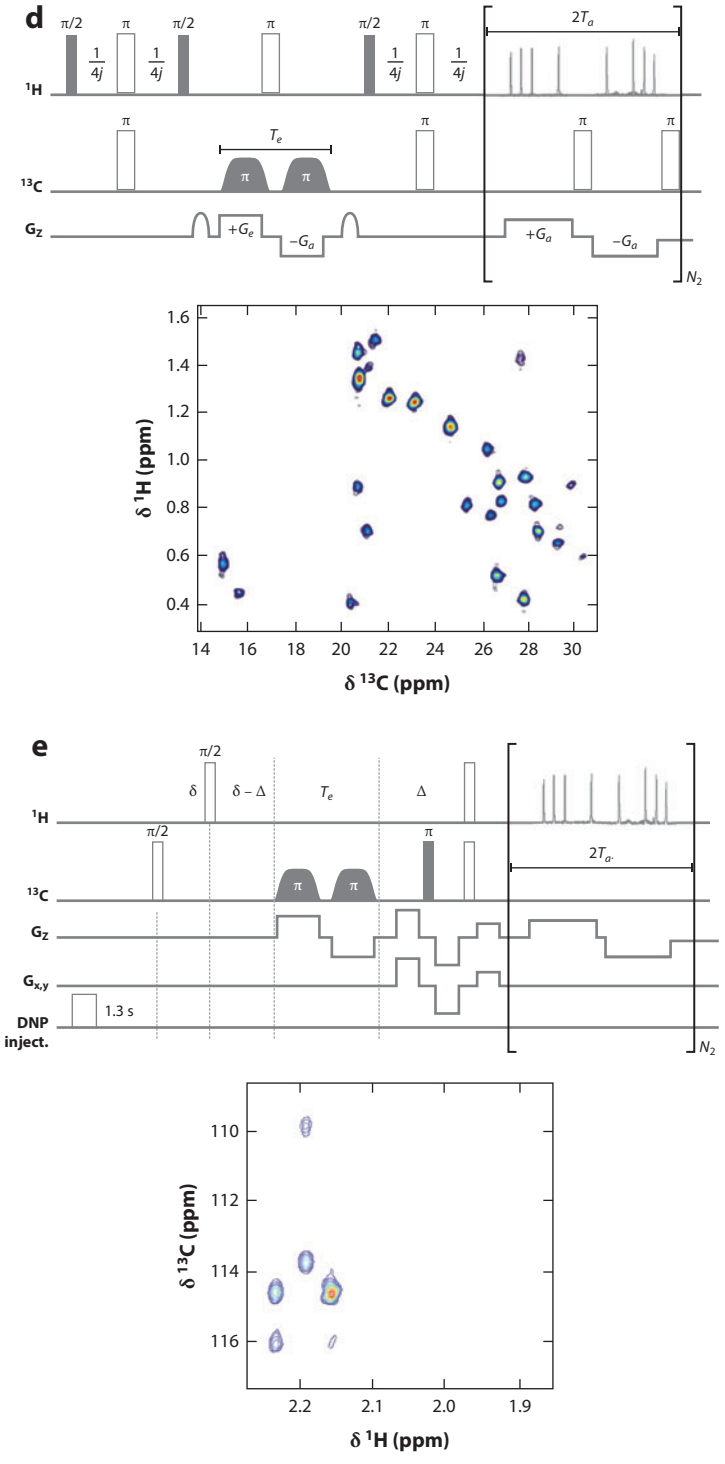

Figure 5

(*Continued*)

lengthier spatiotemporal encoding duration. Other signal-loss/spectral-broadening mechanisms, mainly those arising from the effects of molecular diffusion in the presence of gradients (65, 68) and to a lesser extent from transverse relaxation, limit this possibility. These effects also affect line shapes, in a way that depends on the spatiotemporal encoding scheme (68). Therefore, compromises usually have to be made between resolution along the indirect domain and sensitivity in the 2D spectrum. Finally, a most important sensitivity limitation is given by the need for the method to open up the receiver's bandwidth, so as to succeed in capturing the evolution of two dimensions in a single scan. Indeed, the schemes summarized by **Figures 1–3**, as with their echo planar imaging (EPI) and EPSI counterparts, operate by sampling the full indirect-domain information, within the time period Δt_2 that would normally be associated with the sampling of a single data point in conventional 2D NMR. The larger the direct/indirect-domain spectral widths or the indirect-domain targeted resolution, the more samples will have to be taken, and/or a higher amplitude of the acquisition gradients will be needed and/or shorter sampling times will be required. Any of these circumstances will demand an enhanced sampling rate and thereby an increase of the ensuing spectral noise, which as in any magnetic resonance spectroscopic measurement, increases as the square root of the sampling rate. However, being a single-scan technique, the amount of signal present will be limited to that available in a corresponding single scan of the conventional 2D acquisition counterpart. This is much smaller than the signal arising when a full 2D acquisition is performed, given that a form of signal averaging occurs upon subjecting the latter to a 2D FT (18). Unless special precautions are taken, such as controlled folding, compressed sensing, or other advances mentioned in Section 2.3, below, the signal-to-noise ratio (SNR) in single-scan 2D NMR will be akin to the signal available from a single scan (using the corresponding 2D sequences with all its pulses and coherence transfer processes) scaled by the square root of the number of spectral elements resolved along the indirect domain $\sqrt{SW_1 \cdot t_1{}^{max}}$ (67).

2.3. UF 2D NMR: Advanced Acquisition Considerations

In view of these limitations, research in UF NMR has devoted attention to increase the analytical performance of UF NMR in terms of resolution, sensitivity, and accessible spectral width. Several papers investigated the impact of molecular diffusion on resolution and sensitivity (62, 63, 65, 68), and a multiecho spatiotemporal encoding strategy was proposed for making UF experiments more immune to such effects (62). Diffusion effects can also be reduced by optimizing the sample preparation (69). Modifications of the spatial-encoding period were also proposed for increasing the spectral width that can be observed in the UF dimension without altering resolution, by relying on spectral/spatial pulses (67) or additional gradients (70), to play with the position of peaks in the *k*-space. Recently, the introduction of Hadamard-based strategies in the spatial-encoding schemes also helped to improve its sensitivity (71). Improvements were also brought to the detection scheme by introducing alternative sampling strategies (59, 72). Finally, the processing procedures were also optimized to obtain the best resolution and line shape possible from a given UF data set (73, 74).

One of the key points in the success of a new analytical methodology is its capacity to be easily implemented on routine hardware, even by spectroscopists who would not be specialists of the underlying concepts. Efforts have been targeted to design protocols facilitating such an implementation in the case of UF 2D NMR (60, 75), in particular by designing preacquisition routines to make the setting of experimental parameters easier (76).

Thanks to the numerous improvements described above, the analytical performance of UF NMR has been significantly improved over the past 10 years, and UF NMR has moved from the development stage on model compounds to a powerful analytical tool capable of delivering high-resolution 2D spectra in a fraction of a second. It is now possible to record single-scan spectra

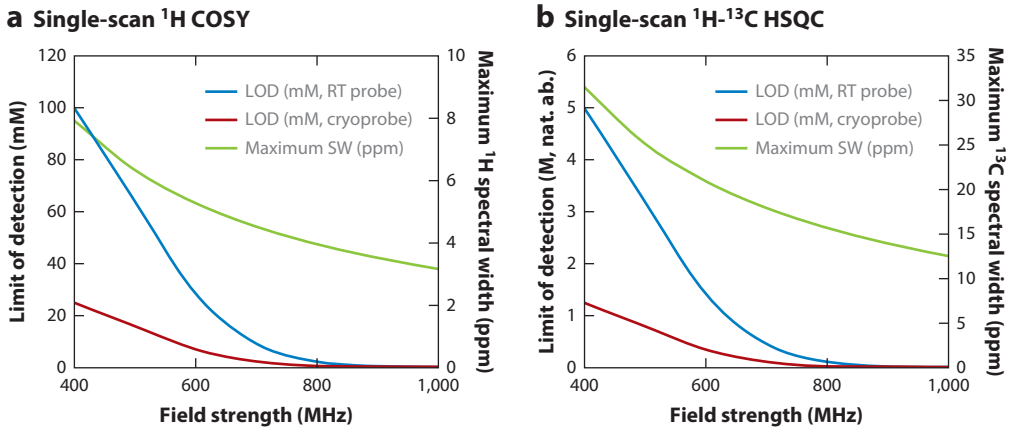

Figure 6

Typical performance of UF (*a*) ^{1}H COSY and (*b*) ^{1}H-^{13}C HSQC experiments on modern NMR hardware. Average approximate values are given, obtained from experimental data and theoretical calculations. Single-scan LODs are given at natural abundance for RT and cryogenic probes. Although these values seem relatively high, the LOD can be easily decreased by signal averaging, as in conventional NMR. The performance of such a multiscan approach is discussed in more detail in the review. Spectral widths are calculated assuming that the spatial-encoding time is $T_e = 30$ ms, which corresponds to a reasonable compromise between resolution and spectral width, and that the maximum gradient amplitude used during acquisition is 30 G/cm. Spectral widths are given regardless of any folding or spectral/spatial manipulation that can further increase the effective observable spectral width. Abbreviations: COSY, correlation spectroscopy; HSQC, heteronuclear single-quantum correlation; LOD, limit of detection; NMR, nuclear magnetic resonance; RT, room temperature; SW, spectral width; UF, ultrafast.

for which the quality is not significantly different from that obtained with their conventional counterparts. Although the first UF experiments were generally limited to pure model molecules, it is now possible to record, in a single scan, 2D spectra of complex diluted mixtures. Of course, there is still a price to pay for the high speed gain, and potential users of UF NMR should be aware of the typical performance that can be reached with these single-scan experiments even on modern hardware. Although this performance is highly spectrometer and probe dependent, **Figure 6** gives typical analytical characteristics of two widely used UF experiments on modern NMR spectrometers. Taking into consideration these factors, readers can assess how these values can possibly translate to their own systems.

3. APPLICATION OF SINGLE-SCAN 2D NMR TO REAL-TIME STUDIES

3.1. Interest of UF 2D NMR for Monitoring Unstable Samples

The recent developments described above have paved the way toward the application of UF NMR to a variety of analytical situations. Not only do UF schemes appear promising to reduce the duration of routine 2D NMR experiments, but their main strength lies in their capacity to solve analytical problems that cannot be addressed by conventional 2D acquisition strategies. This is particularly the case when the timescale of the study is not compatible with the duration of the NMR measurement, for example when samples are subject to chemical or biochemical degradation. It is very likely that samples undergoing second- or minute-long chemical changes cannot be studied by conventional 2D spectroscopy where at least 10 min are required to record a single spectrum. Of course, simple samples can be studied by single-scan conventional 1D NMR,

but numerous cases require the use of 2D spectroscopy, and in this case the use of fast acquisition techniques becomes indispensable.

Total correlation spectroscopy (TOCSY): a common type of homonuclear 2D experiment showing connectivities between all the spins belonging to the same spin system

In this context, numerous studies have demonstrated the potential of UF 2D NMR for monitoring fast processes. An early proof of such a real-time capability was shown by Shapira & Frydman (77), who employed a combination of gradients to monitor, within a single acquisition, the interconversion of *N*,*N*-dimethylacetamide between its two rotamers. This was a dynamic process occurring on a timescale of approximately 1 s. Besides this equilibrium demonstration, real-time monitoring of unidirectional chemical transformations by UF 2D NMR was illustrated in Reference 78 for two examples. The first one followed an H/D exchange process occurring upon dissolving a protonated protein in D_2O, relying on a train of 2D ^{1}H-^{15}N HSQC spectra separated by 4-s intervals. The second one was the real-time in situ tracking of a transient Messenheimer complex that formed rapidly when mixing two reactants inside the NMR tube. By monitoring changes in a series of 2D total correlation spectroscopy (TOCSY) patterns, a competition between thermodynamic and kinetic controls could be observed on a 2-s timescale. The first studies described above anticipated what would be the two main application areas of such real-time approaches: the monitoring of fast organic reactions and the dynamic study of biomolecular processes.

3.2. Monitoring Fast Organic Reactions by UF 2D NMR

UF 2D NMR is particularly promising for the real-time study of organic processes: real-time 1D NMR is a well-known tool for identifying and characterizing intermediates involved in chemical reactions and therefore for understanding reaction mechanisms (79, 80); 2D spectroscopy could naturally enhance such advantages. Herrera et al. (81), for example, first applied the ^{1}H TOCSY approach to follow the synthesis of alkylpyrimidines, observing the reaction between carbonyl compounds and a strong electrophile, trifluoromethanesulfonic acid anhydride (Tf_2O), in the presence of nitriles. 2D spectra were recorded every 10 s over a 90-min time period, allowing the characterization of several intermediates. The real-time monitoring of this multistep reaction revealed important data about its mechanistic and kinetic aspects, which would not have been accessible by conventional means. To obtain further information on the carbonyl carbon atoms involved in this kind of reaction, the same authors proposed a heteronuclear long-distance correlation approach, UF HMBC, to monitor changes involving the nonprotonated carbon atoms. It was a applied to a model ^{13}C-labeled ketone and gave important structural and mechanistic information about the chemical environment and evolution of the reactive nonprotonated carbon (82).

Although the heteronuclear approach described above provides an efficient new tool for the study of complex organic reactions, it is still limited to labeled compounds or relatively high concentrations, thus limiting its applicability. Fortunately, the recent improvements to the sensitivity and robustness of UF pulse sequences have made it possible to extend this approach to ^{13}C studies at natural abundance and lower concentrations. The first demonstration on the potential of the ^{1}H-^{13}C HSQC pulse sequence to monitor organic reactions at natural abundance was performed on a model educational example, namely the mutarotation of glucose in aqueous solution (83). A quantitative treatment of HSQC spectra recorded every 90 s over a 3-h period made it possible to determine the kinetic and equilibrium constants with good precision. Herrera and coworkers (84) applied this natural abundance HSQC strategy to obtain additional mechanistic details in their synthesis of alkylpyrimidines. The complexity of the reaction studied required the development of new UF 2D methods capable of monitoring multiple spectral regions of interest as the reaction progressed. The alternate application of these acquisitions in an interleaved, excitation-optimized fashion allowed extracting new structural and dynamic insights (**Figure 7**). Up to 2,500 2D NMR data sets were collected over the course of this nearly 100-min-long reaction, in an approach

resembling that used in functional MRI. In the same year, the potential of UF 2D NMR to characterize reaction intermediates was illustrated by Queiroz et al. (85), who studied the real-time hydrolysis of an acetal by ^{1}H-^{13}C UF HSQC at natural abundance and were able to characterize the very unstable hemiacetal intermediate with a short lifetime. The results of this study were confirmed and rationalized by quantum calculations of ^{1}H and ^{13}C NMR chemical shifts and natural bonding orbital analysis.

SOFAST: a fast 2D NMR acquisition technique based on optimized relaxation delays and pulse flip angles

3.3. Applications of UF 2D NMR to the Study of Biomolecular Dynamic Processes

NMR is also a widely employed analytical tool in the field of biochemistry, thanks to its capacity to provide structural and dynamic information on biological macromolecules in solution. The investigation of short-lived excited states is greatly important for understanding molecular folding, misfolding, and function, but it remains a challenge for modern biomolecular NMR techniques. Off-equilibrium real-time kinetic NMR can enable the direct observation of conformational or chemical changes; to achieve this, however, multidimensional methods, which are incompatible with the timescale of the targeted phenomena, are often required. UF 2D NMR provides a solution to study such fast dynamic processes. However, the latter often occur on a seconds timescale, which requires a high-repetition rate of NMR experiments, thus seemingly more challenging than the organic reaction monitoring examples discussed above. Initial UF experiments were not compatible with such a repetition rate, due to the interference between the heteronuclear decoupling pulses and the oscillatory magnetic field gradients applied during the acquisition. To circumvent this limitation, Schanda & Brutscher (29) and Frydman and coworkers (86) proposed combining the UF 2D NMR acquisition scheme with the SOFAST technique, recently proposed for increasing the repetition rate of biomolecular NMR experiments. In combination with a fast mechanical mixing device, the recording of ^{1}H-^{15}N correlation spectra with repetition rates of up to a few Hertz became feasible, enabling real-time studies of protein kinetics occurring on timescales down to a few seconds (87).

Recently, this ultraSOFAST approach was applied to follow, in real time, the conformational transitions and structural rearrangements of the adenine-induced folding of an adenine-sensing riboswitch (88). The latter are genetic control elements found in untranslated regions of prokaryotic mRNAs. By following changes in 2D spectra at rates of approximately 0.5 Hz, the authors were able to identify distinct steps associated with the ligand-induced folding of the riboswitch (**Figure 8**).

4. QUANTITATIVE APPLICATIONS OF UF 2D NMR

4.1. Interest in and Limitations of 2D NMR for Quantitative Analysis

Although the real-time monitoring of fast occurring processes is probably the most obvious application of UF 2D NMR, a less evident but equally promising application of fast 2D techniques relates to quantitative analysis of mixtures. NMR is widely employed as a quantitative tool, with applications in fields such as pharmaceutical analysis (89, 90), metabolic studies (91–93), or the authentication of natural products (94, 95). It is of particular interest in the field of metabolomics, where it often exploits a very standardized 1D ^{1}H NMR protocol associated with statistical analysis (96, 97) to compare samples from different sets. Although this method provides efficient discrimination between samples, it does not allow for the quantification of metabolites responsible for this discrimination. A more targeted strategy—metabolic profiling—consists in identifying and quantifying a few tens of metabolites in unfractionated extracts (92, 97, 98). However, a true quantitative analysis of metabolic samples (i.e., a precise and accurate determination of the analytes' concentrations), is challenged by the high degree of signal overlap characterizing complex

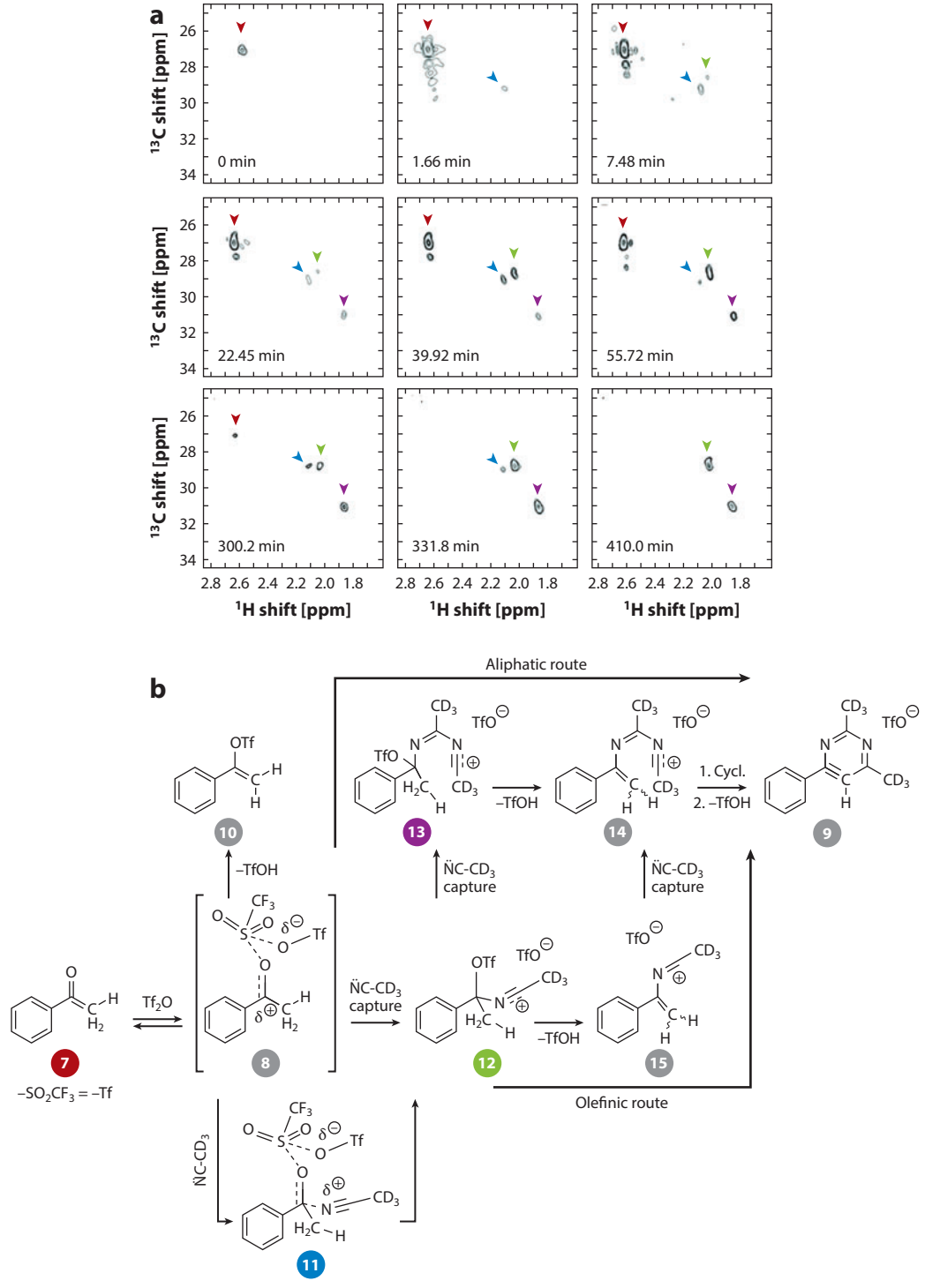

samples. 2D NMR offers promising potential for quantitative analysis of complex mixtures. Its use for quantitative analysis, however, has expanded slowly and only over the past decade (22, 99–109). This reflects one of the main intrinsic characteristics of 2D NMR experiments: their relatively long acquisition times, particularly when seeking quantitative acquisition conditions on large batches of samples. Due to these latter demands, 2D NMR experiments are inherently nonquantitative as peak volumes depend on various factors, mainly relaxation times, J-couplings, and pulse sequence delays, which usually are not extended to the degree that would ensure full relaxation and quantitativeness. This limitation is generally bypassed by relying on a calibration procedure consisting of recording spectra of model mixtures at different concentrations and plotting the peak volumes versus the concentrations for each peak of interest (99, 103, 104, 110, 111). From the quantitative point of view, the main limitation comes from the experimental duration, as long experiments are more likely to be affected by spectrometer instabilities over time (26, 27). They generate additional noise in the indirect dimension, due to the long time interval (several seconds) between the acquisition of two successive points of the pseudo-FID. As a consequence of this so-called t_1 noise, the SNR is always lower in the indirect F_1 dimension, which affects the precision and accuracy of quantitative 2D experiments. This drawback highlights the need for alternative and faster 2D acquisition strategies.

4.2. Interest and Limitations of Quantitative UF 2D NMR

In this context, UF 2D NMR offers promising perspectives for quantitative analysis (108). First, it potentially allows a significant reduction in the experimental duration, which is a significant bonus when considering the relatively long calibration procedures required for quantitative 2D NMR and the frequent need to repeat these for the analysis of several samples. Moreover, UF experiments are potentially more immune to hardware temporal instabilities, as all the t_1 increments are recorded within the same scan. In 2009, Giraudeau et al. (112) performed an analytical evaluation of UF 2D NMR on model mixtures. Two homonuclear UF techniques, J-resolved spectroscopy and TOCSY, were evaluated on model mixtures in terms of repeatability and linearity. Better than 1% repeatability for UF J-resolved spectra and better than 7% for TOCSY spectra was obtained. Moreover, both methods were characterized by an excellent linearity, thus paving way for promising perspectives for this new quantitative methodology called ufo-qNMR (UF optimized quantitative NMR). However, when considering complex mixtures such as those involved in metabolomics studies, the relative sensitivity per unit of time of UF versus conventional 2D NMR needs to be discussed. As mentioned above, a one-scan UF experiment is less sensitive than a conventional experiment where the signal is accumulated during several minutes or hours. A more relevant comparison, however, considers the SNR achieved by these two experiments along the two characterized domains, per unit of time. In other words, for a given experimental acquisition time (e.g., 30 min), should one run a conventional 2D experiment or accumulate complete sets of single-scan UF 2D acquisitions in a multiscan single-shot (M3S) approach? This question is of particular pertinence for metabolic samples that are generally characterized by low concentrations, where averaging several UF experiments will in general be indispensable. To answer this

Figure 7

(*a*) Representative selection of real-time 2D heteronuclear single-quantum correlation NMR spectra arising from the reaction of triflic anhydride, ketone (7), and acetonitrile-d3 shown in panel *b*. Spectra show species (7, 16–18) present in the aliphatic window range (1.54–2.87 ppm for ^{1}H; 23.7–33.7 ppm for ^{13}C) at key time points as the reaction progresses [depicted by arrows (*red*, *blue*, *green*, and *magenta*, respectively)] (84).

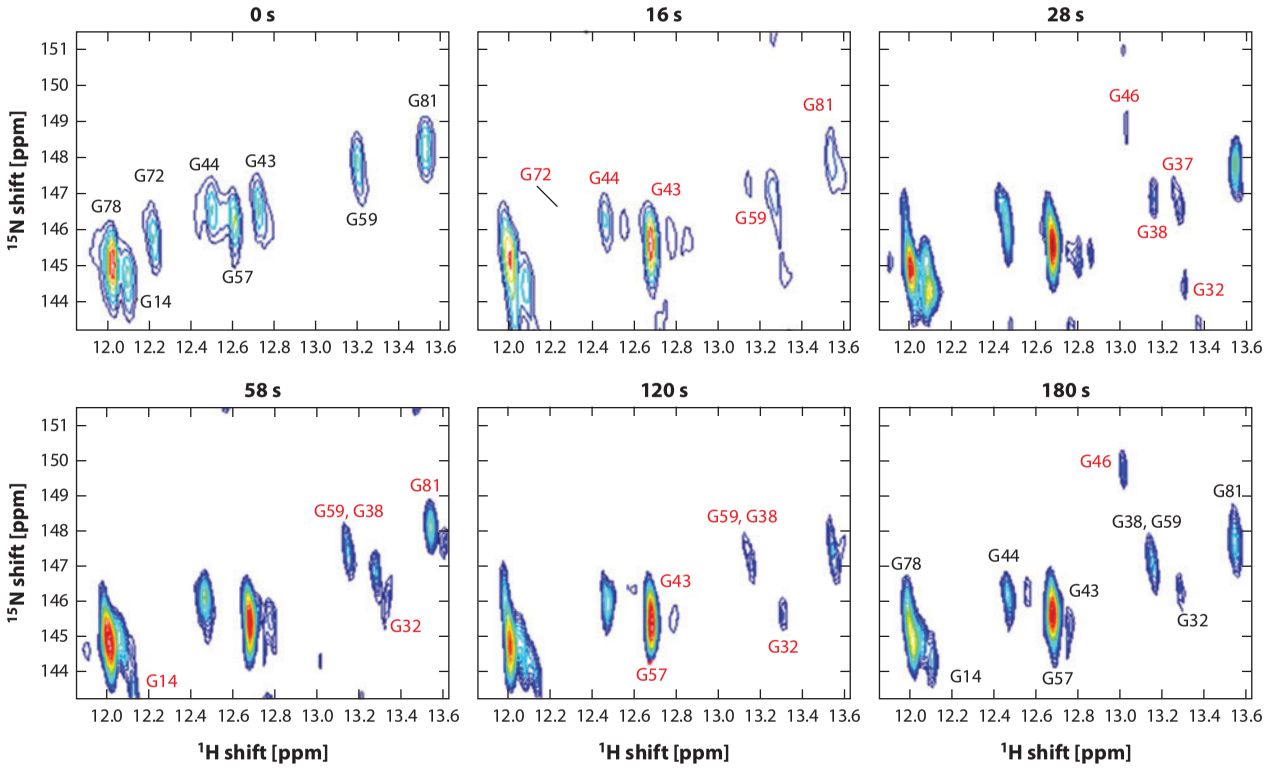

Figure 8

Spectra from Reference 88 illustrating the dynamic capabilities of the ultraSOFAST 2D experiment. Conformational transitions of a riboswitch are followed by recording real-time 2D ^{1}H-^{15}N HMQC NMR spectra. The spectra shown were recorded at pH = 6.1 and 298 K on a ~1.7-mM ^{15}N-G-labeled adenine riboswitch ligand-binding domain; the times indicated in each frame correspond to the time point following addition of adenine and Mg^{2+} to the free RNA solution. Abbreviations: HMQC, heteronuclear multiple-quantum correlation; NMR, nuclear magnetic resonance.

question, Pathan et al. (113) recently carried out a systematic analytical study on model mixtures of metabolites. Surprisingly, for the same experimental duration, and in the case of homonuclear 2D NMR, the M3S approach was more sensitive than conventional 2D NMR. This was attributed to the higher immunity of UF experiments to the temporal instabilities of the hardware. As a consequence, high quantitative performance can be expected from this original approach. Indeed, Le Guennec et al. (114) demonstrated, in the case of COSY experiments, that this M3S acquisition strategy offers better analytical performance (precision and linearity) than conventional 2D NMR.

4.3. Application to Metabolic Samples

The quantitative UF strategy just described can also be applied to solve metabolic issues requiring high-precision and high-accuracy 2D NMR measurements. A first demonstration of this was the determination of absolute metabolite concentrations in biological extracts; this is a goal of the highest relevance for determining characteristic biomarkers to fully understand metabolic complexities. Le Guennec et al. (114) applied an optimized UF COSY approach to measure the absolute metabolite concentration in three breast cancer cell line extracts, relying on a standard addition protocol. M3S COSY spectra of such extracts were recorded in 20 min and yielded the absolute concentrations of 14 major metabolites (**Figure 9**). The results revealed significant metabolic differences between cell lines, thus demonstrating the interest of furthering a UF 2D metabolomics approach.

Another recent quantitative application of UF 2D NMR pertains to the field of fluxomics. As demonstrated by Massou, Portais, and coworkers (22, 106) 2D NMR is a promising tool for studying metabolic fluxes by measuring ^{13}C enrichments in complex mixtures of ^{13}C-labeled metabolites. However, the methods reported thus far have been hindered by long experimental durations, which limit the use of 2D NMR as a quantitative fluxomics tool. In order to take advantage of the time saved and higher precision offered by UF 2D NMR, several acquisition strategies for measuring ^{13}C enrichments from single-scan 2D spectra have been recently proposed

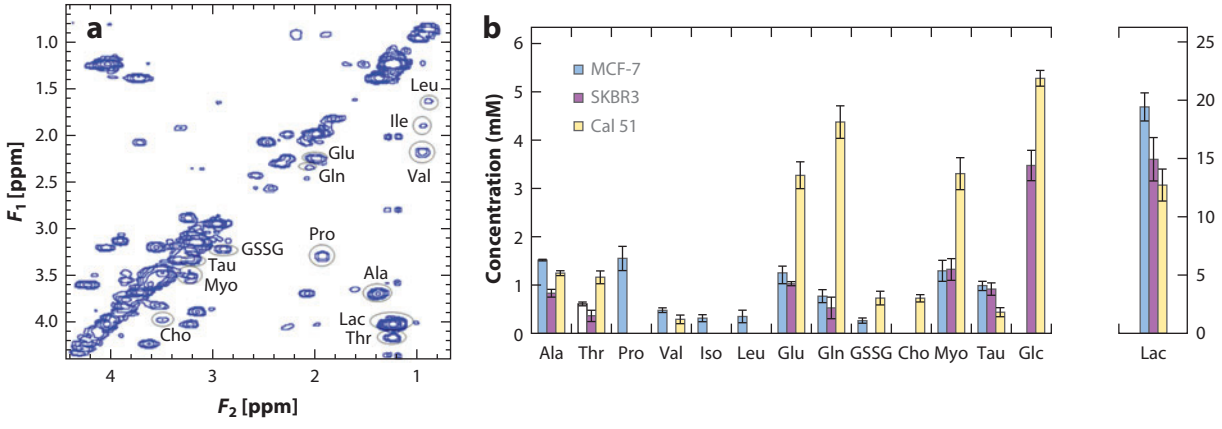

Figure 9

Data extracted from Reference 114, showing the potential of UF 2D NMR for quantitative analysis. (*a*) 2D ^{1}H M3S COSY spectrum of a breast cancer cell line extract, obtained by $CHCl_3$/MeOH/H_2O extraction of breast cancer cells. The spectrum was acquired in 20 min (256 transients). (*b*) Metabolite concentrations of intracellular extracts obtained from three cell lines, SKBR3, MCF-7, and Cal 51, by a quantitative 2D M3S COSY protocol associated with a standard addition procedure. The concentrations are normalized to a 100-mg mass of lyophilized cells. Abbreviations: COSY, correlation spectroscopy; M3S, multiscan single shot; NMR, nuclear magnetic resonance; UF, ultrafast.

(115, 116). Two homonuclear experiments were designed, UF COSY and zTOCSY, where the site-specific ^{13}C enrichments can be measured by reading lines extracted from the 2D spectrum (115). The two approaches were compared in terms of analytical performance, showing accuracy and precision of a few percent and excellent linearity. They were applied to the measurement of ^{13}C enrichments on a biomass hydrolysate (**Figure 10**). The experimental duration was divided by 200 compared to the conventional approach, while yielding the same information on site-specific isotopic enrichments.

5. UF 2D NMR: COUPLING WITH HYPHENATED TECHNIQUES

Coupling NMR with other analytical techniques to increase its separation power—in the case of coupling with chromatography—or its sensitivity—when coupled to hyperpolarization

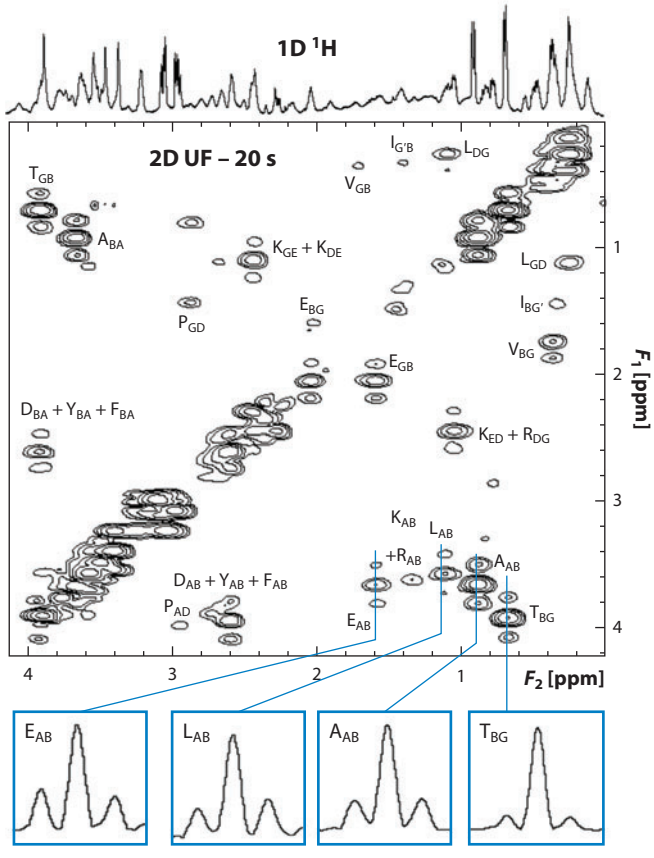

Figure 10

Ultrafast correlation spectroscopy spectrum of a biomass hydrolysate from *E. coli* cells grown on a 1:1 [U-^{13}C]-glucose:glucose mixture (12 g/L). The sample contains mainly amino acids released from the hydrolysis of cellular proteins. The spectrum was recorded in 20 s (4 scans) on a 500-MHz spectrometer equipped with a cryoprobe. Cross-peaks are annotated according to the corresponding carbon in the amino acids, using the international one-letter code for amino acids and standard letters for the position of the protonated carbon in the molecular backbone, i.e., A, B, G, D, and E for α, β, γ, δ, and ε, respectively. Site-specific ^{13}C isotopic enrichments are measured by extracting columns from the 2D spectrum and by integrating the satellites of the resulting site-specific patterns.

techniques—generally involves macroscopic changes in the sample composition over time. It confers upon these experiments an irreversible character, which is incompatible with the time-incremental procedure needed to record 2D spectra. Section 5.1 describes some of the recent advances made that take advantage of the single-scan nature of UF experiments.

Liquid chromatography–nuclear magnetic resonance (LC-NMR): a hyphenated technique consisting of coupling LC with NMR

Dynamic nuclear polarization (DNP): a method to enhance nuclear spin polarization by saturating the resonances of nearby electrons

5.1. UF LC-NMR

Liquid chromatography coupled to nuclear magnetic resonance (LC-NMR) combines the resolving power of chromatography with the structural insight provided by an analytical detection method (117). This efficient technology is becoming increasingly routine worldwide, particularly for pharmaceutical applications (118) and natural product analysis (119). A particularly powerful approach is the on-flow mode, where 1D NMR spectra are obtained as the analytes are eluted from the column. However, such an irreversible process is incompatible with multidimensional NMR methods that form an indispensable tool for the study of complex mixtures. As a consequence, the design and use of fast detection methods is indispensable for performing a real-time 2D NMR characterization of analytes undergoing continuous chromatographic separation. Among the fast 2D NMR methods, only two have been successfully coupled with high-performance liquid chromatography (HPLC). Hadamard spectroscopy was successfully applied in an HPLC-NMR setting (120), an approach which required, however, a priori knowledge of the resonances. Alternatively, Shapira et al. (121) showed the potential of coupling UF NMR with a chromatographic setup to follow the real-time elution of analytes. This study demonstrated the feasibility of such coupling on a home-made experimental setup, consisting of a classical silica-based glass column designed specifically for this kind of experiment. It was applied to model organic compounds in a nonprotonated solvent. More recently, this approach was extended to a commercial HPLC-NMR setup by Queiroz et al. (122). UF COSY spectra were acquired every 12 s in the course of a 12-min chromatographic run performed on a mixture of natural aromatic compounds (**Figure 11**). A noticeable feature was the use of an analytical C-18 column with regular HPLC solvents, demonstrating the applicability of the method to common HPLC-NMR conditions. Although this approach is still hindered by sensitivity losses due to non-negligible flow during spatiotemporal encoding, it paves way for several applications in the numerous fields in which HPLC-NMR can serve as a routine analytical tool.

5.2. UF DNP-NMR

Recent years have witnessed the emergence of different approaches to overcome what is probably the main limitation of NMR, i.e., sensitivity. Several alternatives have been proposed, capable of preparing nuclei in hyperpolarized liquid-phase states. These are metastable spin arrangements in which the bulk nuclear polarizations depart from their usual ($\sim 10^{-5}$) Boltzmann distributions and approach unity values. Once prepared and transferred to an NMR spectrometer, the supersignals that can be elicited from these spin arrangements can be exploited on a timescale dependent on the longitudinal relaxation time T_1 of the hyperpolarized nuclei. Adequate methods proposed and demonstrated for producing and exploiting these extreme spin-polarization levels include the use of parahydrogen (123, 124), the optical pumping of noble gases (125, 126), and microwave-driven dynamic nuclear polarization (DNP) from unpaired electrons (127–129). Among these methods, the last option has the appeal of providing high enhancements with few requirements in terms of chemical substrate or sample preparation. Several in situ (130) or ex situ (129, 131, 132) experimental approaches have been proposed for performing DNP prior to NMR spectroscopic acquisition. Particularly promising have been the metabolic results obtained by the ex situ DNP approach introduced by Golman and coworkers (129), whereby the sample to be analyzed is

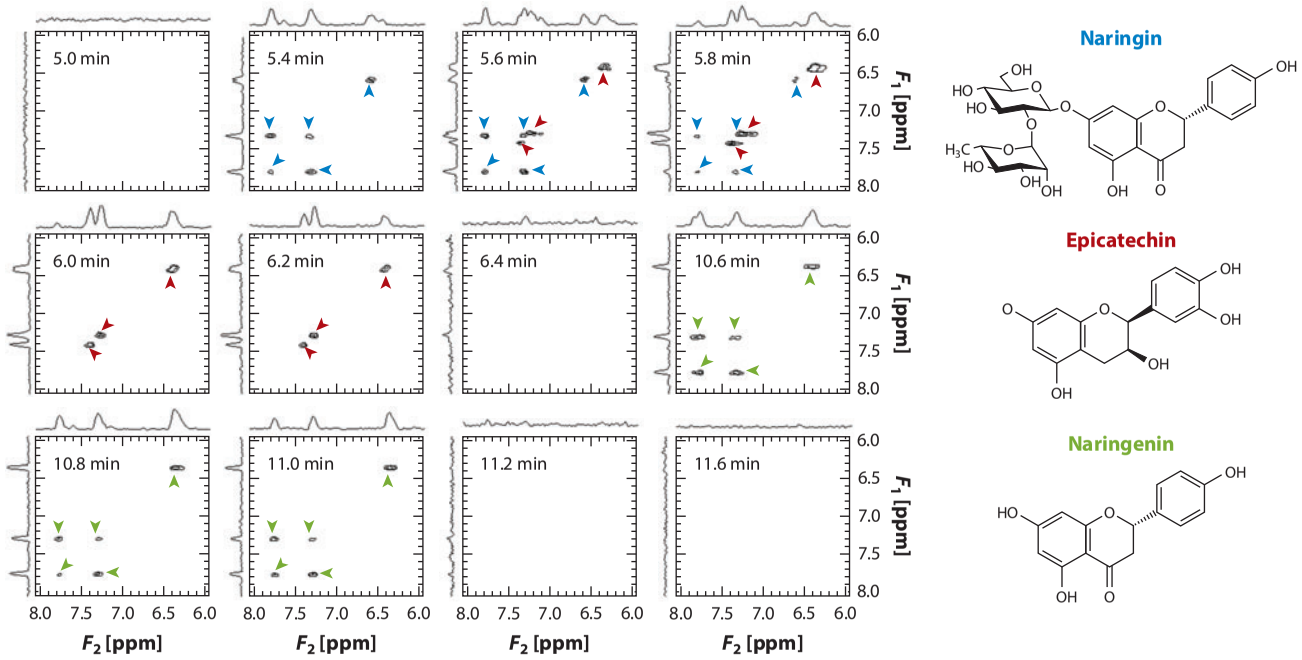

Figure 11

Ultrafast COSY NMR spectra (*aromatic region*) (122) recorded in real time in the course of an HPLC-NMR run on a mixture of naringin (*blue*), epicatechin (*red*), and naringenin (*green*), 10 mg/ml each, dissolved in acetonitrile/water/D_2O 45:27.5:27.5. The spectra were recorded with double solvent presaturation, at 298 K on a 600-MHz Avance III spectrometer equipped with a cryogenic probe, including a cryofit accessory with an active cell volume of 60 μL. Abbreviations: COSY, correlation spectroscopy; HPLC, high-performance liquid chromatography; NMR, nuclear magnetic resonance.

comixed with a free radical, frozen in a glass at cryogenic temperatures, and hyperpolarized by irradiating the radical close to its unpaired electron's Larmor frequency for relatively long periods of time. Rapid melting and shuttling of the nuclear spins from this cryogenic environment to a spectrometer enables an otherwise routine solution-state NMR spectroscopic observation. Upon taking into account the effects of the cryogenic cooling and of the DNP process, these "routine" observations will take place on nuclei, the polarization of which has been enhanced by a factor of approximately 10^4.

Despite its outstanding promise, the irreversible character of ex situ DNP-NMR is best suited for collecting a single or at most a few scans. This makes it a poor starting point for acquiring arrayed transients involving the complex pulse sequences needed to complete conventional 2D NMR acquisitions. A particularly promising solution is to record single-scan 2D NMR spectra of hyperpolarized compounds via UF 2D methods. The potential of this powerful coupling was demonstrated in 2007 by Frydman & Blazina (133), who showed that 2D spectra of hyperpolarized liquid samples at submicromolar concentrations could be acquired within 0.1 s. Their results highlight the high complementarity of the two techniques: UF 2D NMR solves the irreversibility issue of ex situ DNP-NMR, and DNP offers a solution to the relatively low sensitivity of UF 2D NMR.

Another drawback of the ex situ DNP-NMR setting is the time needed to transfer the sample from the polarizer to the NMR spectrometer (*c.a.* 1 s). It implies that only sites with relatively long liquid states T_1 will be able to retain a significant hyperpolarization. Therefore, high performance can be expected from UF 2D methods exploiting the hyperpolarization of slow relaxing, low-γ nuclei such as nonprotonated ^{13}C. This implies using long-distance correlation experiments between nonprotonated ^{13}C and nonbonded protons, such as the HMBC experiment. The UF version of this experiment was successfully coupled with ex situ DNP in 2008 (134), which relied on hyperpolarized quaternary ^{13}C and ^{15}N nuclei. In 2009, band-selective approaches were proposed for the simultaneous recording of several 2D NMR correlations in a single scan, a strategy that was successfully applied to mixtures of hyperpolarized natural products at millimolar concentrations (135) (**Figure 12**).

These recent advances highlight the interest of coupling UF 2D NMR with DNP and pave way for numerous application perspectives. It was also recently shown that UF NMR could not only be successfully coupled within a different DNP setting (136)—allowing faster transfer of the analytes and therefore the acquisition of homonuclear UF 2D experiments—but also with other hyperpolarization methods such as parahydrogen (137).

6. PSEUDO-2D UF NMR

A final group of single-scan methods worth addressing concerns new and emerging techniques that rely on the principles of UF 2D NMR but are not strictly speaking 2D NMR acquisitions, in the sense that they do not entail the encoding of a coherent indirect-domain evolution. Still, these methods are potentially useful in analytical studies, and the possibility to perform them in a UF format could enable their systematic use to study molecular dynamic properties in real time.

One such promising approach consists in the development of fast, spatially encoded methods for the measurement of longitudinal relaxation times (T_1). These determinations can provide a valuable tool for understanding the dynamics of spin systems and for probing molecular motions over a wide range of timescales. The measurement of T_1 generally relies on pseudo-2D experiments such as inversion-recovery (IR) (138), which are hindered by long acquisition times and are therefore beyond the usual scope of real-time studies. Several ideas have been proposed for reducing the duration of IR experiments, such as the slice-selective approaches (139, 140) that make

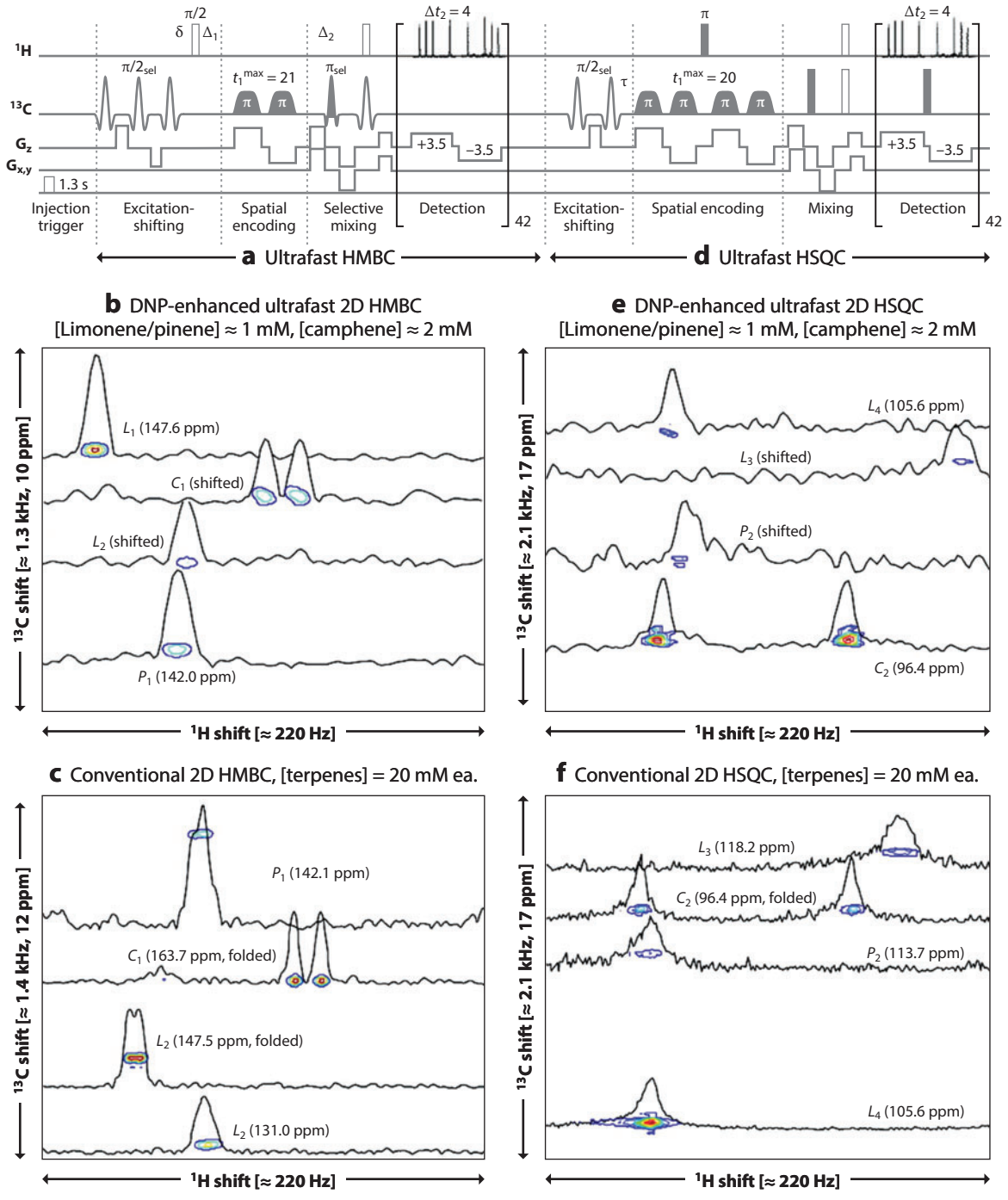

it possible to access small-molecule T_1s in a single scan. Although these methods are better suited for studying long T_1s (typically several seconds), subsecond relaxation times are often observed, particularly when probing dynamic phenomena at the molecular level. Very recently, Smith et al. (141) proposed a pulse sequence akin to UF 2D NMR experiments to perform single-scan IR experiments adapted to short T_1s. It can be considered pseudo-2D UF in the sense that it requires 2D FT of the data, but T_1s are determined from a single-scan experiment, making it possible to study real-time molecular dynamics.

In a similar vein, also worth exploring are the alternative approaches capable of separating analytes via their dynamic properties based on their diffusion coefficients (142). The diffusion-ordered spectroscopy (DOSY) methodology encodes the effect of random Brownian motion in the indirect dimension, thanks to a series of experiments recorded with incremented gradient strength. While DOSY is highly powerful for studying complex mixtures, it still suffers from an incrementation scheme akin to the one of 2D NMR which limits its applicability, particularly when dynamic or unstable systems are studied. A UF version of DOSY was recently described to overcome this drawback (143), based on the intimate relationship between UF spectroscopy and diffusion effects (65, 68). It opens promising perspectives for monitoring diffusion and flow phenomena in complex systems.

In a final example of such pseudo-2D UF strategies, Jerschow and coworkers (144) have recently demonstrated the use of a spatial domain to speed up the study of chemical exchange saturation transfer (CEST) phenomena, which is a popular approach for generating MRI contrast and particularly promising for studying in vivo metabolism. In conventional CEST experiments, the polarization of water is measured as a function of incremented offsets of a saturated RF irradiation (145). In the UF version of this experiment, signals with different irradiation offsets are recorded simultaneously in different parts of the sample, which makes it possible to record a full *Z*-spectrum in only two scans. Although this approach, as with others described above, suffers from a lower sensitivity inherent to the UF approach, it is very promising when coupled with hyperpolarization methods.

Diffusion-ordered spectroscopy (DOSY): a pseudo-2D experiment separating the analytes based on their molecular diffusion properties

Chemical exchange saturation transfer (CEST): a process involving the chemical exchange of a nucleus in the NMR experiment from one site to a chemically different site

7. CONCLUSION AND PERSPECTIVES

This review presents some of the progress made in the field of UF 2D NMR, particularly as it relates to making this spectroscopic method a powerful complement to the NMR analytical toolkit. Thanks to recent developments, this method has the potential for a variety of analytical

Figure 12

Pulse sequences and spectra from Reference 135 showing the potential of coupling UF 2D NMR with ex situ DNP. (*a*,*d*) Successive 2D HMBC and HSQC ^{13}C-^{1}H UF pulse sequences, including gradient and timing parameters (in G/cm and ms) and spectral/spatial manipulations bringing the relevant signals inside the targeted spectral window. (*b*,*e*) UF HMBC and HSQC 2D spectra with relevant cross sections obtained after polarizing 4.4 μL of a 0.5-M limonene/α-pinene/camphene 1:1:2 solution in a toluene/toluene-d8 1:5 mixture with 20-mM BDPA. Sudden dissolution in methanol-d4 led to a final concentration of 1 mM for limonene and α-pinene, and 2 mM for camphene. (*c*,*f*) Conventional HMBC and HSQC 2D NMR spectra collected on a 20-mM equimolar terpene mixture in $CDCl_3$, obtained in 90 min using 32 scans, 64 t_1 increments, a 2-s recycle delay, and a 0.5-s acquisition time. These conventional data were acquired with the same ^{13}C spectral widths as the UF spectra, leading to the aliasing of some of the peaks. Also shown are the unfolded positions of the ^{13}C resonances characterized in each experiment (in ppm from TMS). Both HSQC and HMBC conventional pulse sequences were made spectrally selective to avoid the appearance of unwanted ^{13}C resonances. Abbreviations: BDPA, α,γ-bisdiphenylene-β-phenylallyl; DNP, dynamic nuclear polarization; HMBC, heteronuclear multiple-bond correlation; HSQC, heteronuclear single-quantum correlation; NMR, nuclear magnetic resonance; TMS, tetramethylsilane; UF, ultrafast.

applications, from the real-time monitoring of chemical and biochemical processes to the quantitative analysis of metabolic samples. Although sensitivity appears to be a key limitation of this methodology, SNR increases of several orders of magnitude can be expected from its coupling with hyperpolarization techniques. Such coupling could particularly benefit the quantitative analysis of metabolic samples, where recent results obtained with UF 2D NMR have paved way for exciting perspectives, except where analyte concentration is low, which is often an issue. Research perspectives will include the design of analytical strategies to accurately measure metabolite concentrations from 2D NMR spectra following DNP. When considering complex metabolic samples, where even 2D spectra may be hampered by peak overlap, significant improvement can be expected from the development of approaches with higher dimensionality. Although pure UF 3D NMR approaches are feasible in practice (146), their resolution and sensitivity drawbacks become even more severe than those of the normal 2D UF NMR counterparts. On the other hand,

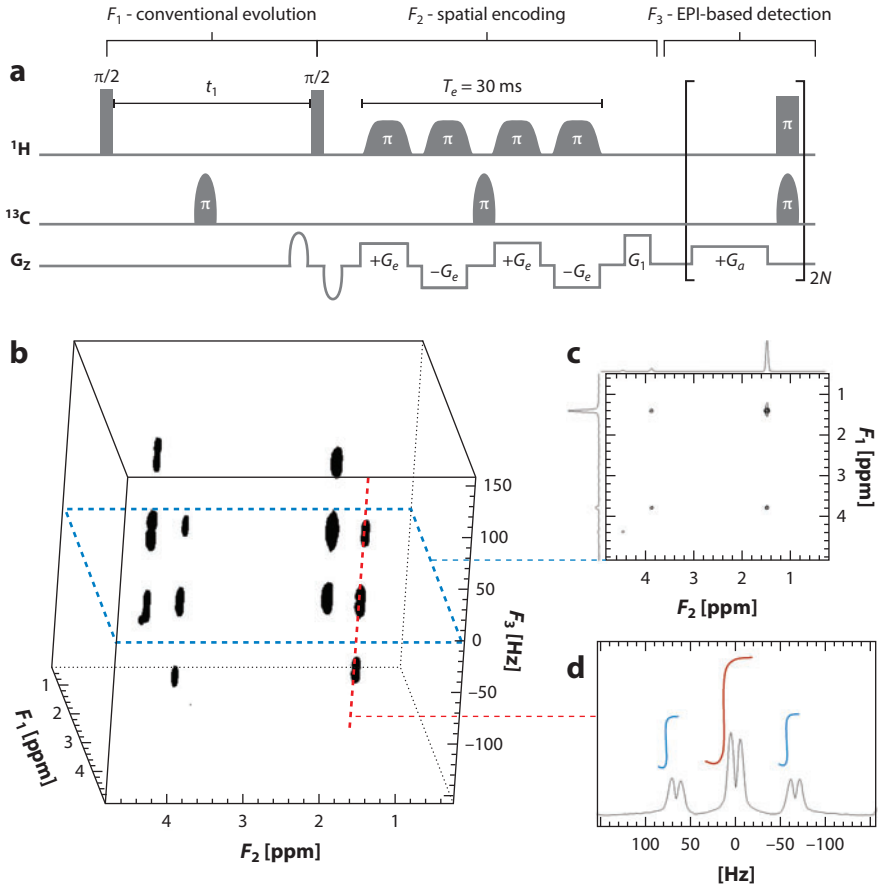

Figure 13

(*a*) 3D UF JCOSY pulse sequence and corresponding (*b*) 3D NMR spectrum of a ^{13}C-labeled alanine sample (147) capable of recording a 3D JCOSY in 11 min relying on a hybrid conventional-UF acquisition strategy. (*c*) A F_1F_2 plane read from the 3D spectrum gives rise to a COSY-type correlation, where the peaks are not broadened by heteronuclear couplings in spite of the ^{13}C enrichment. (*d*) The heteronuclear couplings are obtained from dimension F_3, and the ^{13}C isotopic enrichments are measured by reading a column perpendicular to the COSY plane. Abbreviations: JCOSY, COSY-J-resolved spectrum; UF, ultrafast.

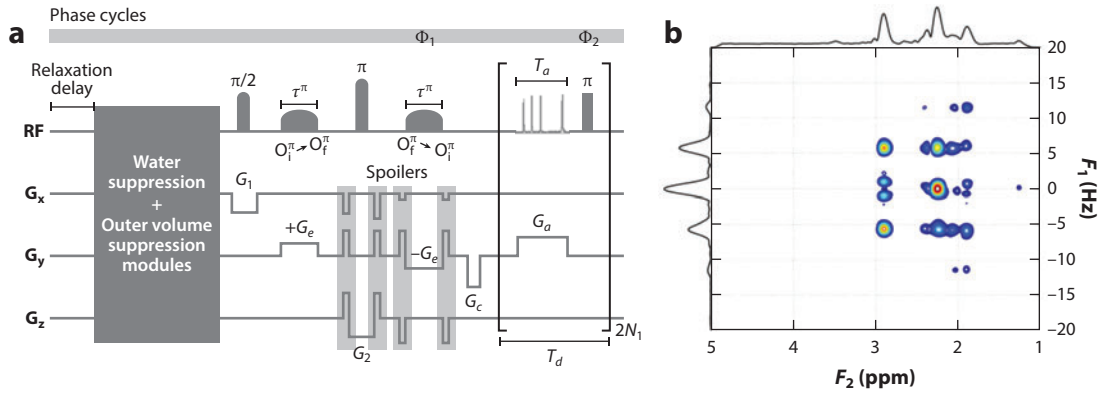

Figure 14

(*a*) UF JPRESS pulse sequence capable of recording 3D-localized, 2D J-resolved UF spectra on a small animal imaging system. (*b*) Corresponding spectrum acquired in 2 min 40 s on an in vitro phantom containing a GABA solution (10% w/w in water) placed at the center of a 50 mL tube of pure ethanol. The spectrum was recorded on a 7T imaging system (small animal). Abbreviations: GABA, gamma-aminobutyric acid; JPRESS, J-resolved point-resolved spectroscopy; UF, ultrafast.

high spectral qualities have been demonstrated from hybrid conventional/UF 3D approaches capable of recording a whole 3D spectrum in the time needed to record a conventional 2D spectrum. This strategy was first suggested in a biomolecular context (66) and was recently applied successfully to the measurement of site-specific ^{13}C isotopic enrichments (147) (**Figure 13**).

Finally, promising perspectives also arise from the extension of the UF methodology to the field of in vivo spectroscopy, where considerable gains can be expected from the speed gain offered by the single-scan approach. A first step toward localized spectroscopy was recently taken by Roussel et al. (148), who proposed an approach capable of recording UF 2D J-resolved localized spectra on in vitro phantoms placed in a small animal imaging system (**Figure 14**). The application of UF spectroscopy to in vivo systems sounds particularly promising when considering the recent work of Pelupessy et al. (149) and Zhang et al. (150), who recently designed single-scan approaches capable of recording high-resolution 2D spectra in the presence of spatial inhomogeneities, which is a central issue in the field of in vivo spectroscopy.

Finally, the success of a new methodology also lies in its capacity to be implemented by a wide range of users in academic or industrial research labs. Although UF NMR is not yet a push-button technique, recent efforts have considerably increased its accessibility, and hopefully it's just a matter of time before manufacturers begin to implement it on commercial spectrometers.

DISCLOSURE STATEMENT

The authors are not aware of any affiliations, memberships, funding, or financial holdings that might be perceived as affecting the objectivity of this review.

ACKNOWLEDGMENTS

Patrick Giraudeau thanks the French National Research Agency for a Young Investigator starting grant (ANR grant 2010-JCJC-0804-01), as well as Professor Serge Akoka for helpful discussions. Lucio Frydman acknowledges the Israel Science Foundation (projects ISF 795/13 and iCore grant 1775/12), ERC Advanced grant 246754, EU's BioNMR grant 261863, a Helen and Kimmel Award for Innovative Investigation, and the generosity of the Perlman Family Foundation.

LITERATURE CITED

1. Batta G, Kovir K, Jossuth L, Szankey C. 1997. Methods of structure elucidation by high-resolution NMR. In *Analytical Spectroscopy Library*, pp. 1–357. London: Elsevier
2. Simpson JH. 2008. *Organic Structure Determination Using 2-D NMR Spectroscopy: A Problem-Based Approach*. San Diego, CA: Academic
3. Cavanagh J, Fairbrother WJ, Palmer AG, Skelton NJ, Rance M. 2006. *Protein NMR Spectroscopy: Principles and Practice*. Amsterdam: Elsevier
4. Wüthrich K. 1986. *NMR of Proteins and Nucleic Acids*. New York: Wiley
5. Tycko R, ed. 2003. *Nuclear Magnetic Resonance Probes of Molecular Dynamics*. Dordrecht, Ger.: Springer
6. Jeener J. 1971. *Lecture presented at Ampere International Summer School II, Basko Polje, Yugoslavia*
7. Aue WP, Bartholdi E, Ernst RR. 1976. Two-dimensional spectroscopy. Application to nuclear magnetic resonance. *J. Chem. Phys.* 64:2229–46
8. Derome AE. 1987. *Modern NMR Techniques for Chemistry Research*. Oxford, UK: Pergamon
9. Deleted in proof
10. Maudsley AA, Ernst RR. 1977. Indirect detection of magnetic resonance by heteronuclear two-dimensional spectroscopy. *Chem. Phys. Lett.* 50:368–72
11. Müller L, Kumar A, Ernst RR. 1977. Two-dimensional carbon-13 spin-echo spectroscopy. *J. Magn. Reson.* 25:383–90
12. Jeener J, Meier BH, Bachmann P, Ernst RR. 1979. Investigation of exchange processes by two-dimensional NMR spectroscopy. *J. Chem. Phys.* 72:4546–53
13. Bodenhausen G, Ruben DJ. 1980. Natural abundance nitrogen-15 NMR by enhanced heteronuclear spectroscopy. *Chem. Phys. Lett.* 69:185–89
14. Bax A, Griffey RH, Hawkins BL. 1983. Correlation of proton and nitrogen-15 chemical shifts by multiple quantum NMR. *J. Magn. Reson.* 55:301–15
15. Bax A, Summers MF. 1986. Proton and carbon-13 assignments from sensitivity-enhanced detection of heteronuclear multiple-bond connectivity by 2D multiple quantum NMR. *J. Am. Chem. Soc.* 108:2093–94
16. Aue WP, Bachmann P, Wokaun A, Ernst RR. 1978. Sensitivity of two-dimensional NMR spectroscopy. *J. Magn. Reson.* 29:523–33
17. Aue WP, Karhan J, Ernst RR. 1976. Homonuclear broad band decoupling and two-dimensional J-resolved NMR spectroscopy. *J. Chem. Phys.* 64:4226–27
18. Ernst RR, Bodenhausen G, Wokaun A. 1987. *Principles of Nuclear Magnetic Resonance in One and Two Dimensions*. Oxford, UK: Clarendon Press
19. Topcu G, Ulubelen A. 2007. Structure elucidation of organic compounds from natural sources using 1D and 2D NMR techniques. *J. Mol. Struct.* 834:57–73
20. Li D, Owen NL, Perera P, Andersson C, Bohlin L, et al. 1994. Structure elucidation of three triterpenoid saponins from *Alphitonia zizyphoides* using 2D NMR techniques. *J. Nat. Prod.* 57:218–24
21. Koskela H. 2009. Quantitative 2D NMR studies. *Annu. Rep. NMR Spectrosc.* 66:1–31
22. Massou S, Nicolas C, Letisse F, Portais J-C. 2007. NMR-based fluoxomics: quantitative 2D NMR methods for isotopomers analysis. *Phytochemistry* 68:2330–40
23. Englander SW, Mayne L. 1992. Protein folding studied using hydrogen-exchange labeling and two-dimensional NMR. *Annu. Rev. Biophys. Biomol. Struct.* 21:243–65
24. Machonkin TE, Westler WM, Markley JL. 2002. $^{13}C\{^{13}C\}$ 2D NMR: a novel strategy for the study of paramagnetic proteins with slow electronic relaxation rates. *J. Am. Chem. Soc.* 124:3204–5
25. Kriwacki RW, Pitner TP. 1989. Current aspects of practical two-dimensional (2D) nuclear magnetic resonance (NMR) spectroscopy: applications to structure elucidation. *Pharm. Res.* 6:531–54
26. Mehlkopf AF, Korbee D, Tiggelman TA, Freeman R. 1984. Sources of t_1 noise in two-dimensional NMR. *J. Magn. Reson.* 58:315–23
27. Morris GA. 1992. Systematic sources of signal irreproducibility and t_1 noise in high-field NMR spectrometers. *J. Magn. Reson.* 100:316–28
28. Ross A, Salzmann M, Senn H. 1997. Fast-HMQC using Ernst angle pulses: an efficient tool for screening of ligand binding to target proteins. *J. Biomol. NMR* 10:389–96

29. Schanda P, Brutscher B. 2005. Very fast two-dimensional NMR spectroscopy for real-time investigation of dynamic events in proteins on the time scale of seconds. *J. Am. Chem. Soc.* 127:8014–15
30. Cai S, Seu C, Kovacs Z, Sherry AD, Chen Y. 2006. Sensitivity enhancement of multidimensional NMR experiments by paramagnetic relaxation effects. *J. Am. Chem. Soc.* 128:13474–78
31. Vitorge B, Bodenhausen G, Pelupessy P. 2010. Speeding up nuclear magnetic resonance spectroscopy by the use of SMAll Recovery Times—SMART NMR. *J. Magn. Reson.* 207:149–52
32. Jeannerat D. 2003. High resolution in heteronuclear ^{1}H-^{13}C NMR experiments by optimizing spectral aliasing with one-dimensional carbon data. *Magn. Reson. Chem.* 41:3–17
33. Donoho DL, Tsaig Y. 2008. Fast solution of l_1-norm minimization problems when the solution may be sparse. *IEEE* 54:4789–812
34. Stern AS, Donoho DL, Hoch JC. 2007. NMR data processing using iterative thresholding and minimum l_1-norm reconstruction. *J. Magn. Reson.* 188:295–300
35. Barkhuijsen H, De Beer R, Bovée WMMJ, Van Ormondt D. 1985. Retrieval of frequencies, amplitudes, damping factors, and phases from time-domain signals using a linear least-squares procedure. *J. Magn. Reson.* 61:465–81
36. Stern AS, Li K-B, Hoch JC. 2002. Modern spectrum analysis in multidimensional NMR spectroscopy: comparison of linear-prediction extrapolation and maximum-entropy reconstruction. *J. Am. Chem. Soc.* 124:1982–93
37. Hoch JC. 1985. Maximum entropy signal processing of two-dimensional NMR data. *J. Magn. Reson.* 64:436–40
38. Kazimierczuk K, Zawadzka A, Koźmiński W. 2008. Optimization of random time domain sampling in multidimensional NMR. *J. Magn. Reson.* 192:123–30
39. Brüschweiler R, Zhang F. 2004. Covariance nuclear magnetic resonance spectroscopy. *J. Chem. Phys.* 120:5253–60
40. Barna JCJ, Laue ED, Mayger MR, Skilling J, Worrall SJP. 1987. Exponential sampling, an alternative method for sampling in two-dimensional NMR experiments. *J. Magn. Reson.* 73:69–77
41. Kupce E, Freeman R. 2005. Fast multidimensional NMR: radial sampling of evolution space. *J. Magn. Reson.* 173:317–21
42. Kamzimierczuk K, Zawadzka A, Koźmiński W, Zhukov I. 2007. Lineshapes and artifacts in multidimensional Fourier Transform of arbitrary sampled NMR data sets. *J. Magn. Reson.* 188:344–56
43. Lafon O, Hu B, Amoureux J-P, Lesot P. 2011. Fast and high-resolution stereochemical analysis by nonuniform sampling and covariance processing of anisotropic natural abundance 2D 2H NMR datasets. *Chem. Eur. J.* 17:6716–24
44. Kupce E, Freeman R. 2003. Two-dimensional Hadamard spectroscopy. *J. Magn. Reson.* 162:300–10
45. Frydman L, Lupulescu A, Scherf T. 2003. Principles and features of single-scan two-dimensional NMR spectroscopy. *J. Am. Chem. Soc.* 125:9204–17
46. Frydman L, Scherf T, Lupulescu A. 2002. The acquisition of multidimensional NMR spectra within a single scan. *Prod. Natl. Acad. Sci. USA* 99:15858–62
47. Mansfield P. 1977. Multi-planar image formation using NMR spin echoes. *J. Phys. C* 10:55–58
48. Mansfield P. 1984. Spatial mapping of the chemical shift in NMR. *Magn. Reson. Med.* 1:370–86
49. Shrot Y, Frydman L. 2003. Ghost-peak suppression in ultrafast two-dimensional NMR spectroscopy. *J. Magn. Reson.* 164:351–57
50. Pelupessy P. 2003. Adiabatic single scan two-dimensional NMR spectroscopy. *J. Am. Chem. Soc.* 125:12345–50
51. Shrot Y, Shapira B, Frydman L. 2004. Ultrafast 2D NMR spectroscopy using a continuous spatial encoding of the spin interactions. *J. Magn. Reson.* 171:163–70
52. Andersen NS, Köckenberger W. 2005. A simple approach for phase-modulated single-scan 2D NMR spectroscopy. *Magn. Reson. Chem.* 43:791–94
53. Tal A, Shapira B, Frydman L. 2005. A continuous phase-modulated approach to spatial encoding in ultrafast 2D NMR spectroscopy. *J. Magn. Reson.* 176:107–14
54. Shapira B, Shrot Y, Frydman L. 2006. Symmetric spatial encoding in ultrafast 2D NMR spectroscopy. *J. Magn. Reson.* 178:33–41

55. Shrot Y, Frydman L. 2008. Spatial encoding strategies for ultrafast multidimensional nuclear magnetic resonance. *J. Chem. Phys.* 128:052209
56. Wu C, Zhao M, Cai S, Lin Y, Chen Z. 2010. Ultrafast 2D COSY with constant-time phase-modulated spatial encoding. *J. Magn. Reson.* 204:82–90
57. Basus VJ, Ellis PD, Hill HDW, Waugh JS. 1979. Utilization of chirp frequency modulation for heteronuclear spin decoupling. *J. Magn. Reson.* 35:19–37
58. Böhlen JM, Bodenhausen G. 1992. Experimental aspects of chirp NMR spectroscopy. *J. Magn. Reson. A* 102:293–301
59. Giraudeau P, Akoka S. 2007. A new detection scheme for ultrafast 2D *J*-resolved spectroscopy. *J. Magn. Reson.* 186:352–57
60. Gal M, Frydman L. 2010. Ultrafast multidimensional NMR: principles and practice of single-scan methods. In *Encyclopedia of Magnetic Resonance*, ed. GA Morris, JW Emsley, pp. 43–60. Chichester, UK: Wiley
61. Tal A, Frydman L. 2010. Single-scan multidimensional magnetic resonance. *Prog. Nucl. Magn. Reson. Spectrosc.* 57:241–92
62. Giraudeau P, Akoka S. 2008. Resolution and sensitivity aspects of ultrafast 2D *J*-resolved 2D NMR spectra. *J. Magn. Reson.* 190:339–45
63. Giraudeau P, Akoka S. 2008. Sources of sensitivity losses in ultrafast 2D NMR. *J. Magn. Reson.* 192:151–58
64. Pelupessy P, Duma L, Bodenhausen G. 2008. Improving resolution in single-scan 2D spectroscopy. *J. Magn. Reson.* 194:169–74
65. Shrot Y, Frydman L. 2008. The effects of molecular diffusion in ultrafast two-dimensional nuclear magnetic resonance. *J. Chem. Phys.* 128:164513
66. Mishkovsky M, Frydman L. 2009. Principles and progress in ultrafast multidimensional nuclear magnetic resonance. *Annu. Rev. Phys. Chem.* 60:429–48
67. Shrot Y, Frydman L. 2009. Spatial/spectral encoding of the spin interactions in ultrafast multidimensional NMR. *J. Chem. Phys.* 131:224516
68. Giraudeau P, Akoka S. 2008. Sensitivity losses and line shape modifications due to molecular diffusion in continuous encoding ultrafast 2D NMR experiments. *J. Magn. Reson.* 195:9–16
69. Rouger L, Loquet D, Massou S, Akoka S, Giraudeau P. 2012. Limitation of diffusion effects in ultrafast 2D NMR by encapsulation of analytes in phospholipidic vesicles. *Chem. Phys. Chem.* 13:4124–27
70. Giraudeau P, Akoka S. 2010. A new gradient-controlled method for improving the spectral width of ultrafast 2D NMR experiments. *J. Magn. Reson.* 205:171–76
71. Tal A, Shapira B, Frydman L. 2009. Single-scan 2D Hadamard NMR spectroscopy. *Angew. Chem. Int. Ed.* 48:2732–36
72. Shrot Y, Frydman L. 2011. Compressed sensing and the reconstruction of ultrafast 2D NMR data: principles and biomolecular applications. *J. Magn. Reson.* 209:352–58
73. Mishkovsky M, Frydman L. 2005. Interlaced Fourier transformation of ultrafast 2D NMR data. *J. Magn. Reson.* 173:344–50
74. Giraudeau P, Akoka S. 2011. Sensitivity and lineshape improvement in ultrafast 2D NMR by optimized apodization in the spatially encoded dimension. *Magn. Reson. Chem.* 49:307–13
75. Queiroz LHK Jr, Ferreira AG, Giraudeau P. 2013. Optimization and practical implementation of ultrafast 2D NMR experiments. *Quim. Nova.* 26:577–81
76. Pathan M, Charrier B, Tea I, Akoka S, Giraudeau P. 2013. New practical tools for the implementation and use of ultrafast 2D NMR experiments. *Magn. Reson. Chem.* 51:168–75
77. Shapira B, Frydman L. 2003. Arrayed acquisition of 2D exchange NMR spectra within a single scan experiment. *J. Magn. Reson.* 165:320–24
78. Gal M, Mishkovsky M, Frydman L. 2006. Real-time monitoring of chemical transformations by ultrafast 2D NMR spectroscopy. *J. Am. Chem. Soc.* 128:951–56
79. Li W, Li J, Wu Y, Fuller N, Markus MA. 2010. Mechanistic pathways in CF_3COOH-mediated deacetalization reactions. *J. Org. Chem.* 75:1077–86

80. Bussy U, Giraudeau P, Silvestre V, Jaunet-Lahary T, Ferchaud-Roucher V, et al. 2013. In situ NMR spectroelectrochemistry for the structure elucidation of unstable intermediate metabolites. *Anal. Bioanal. Chem.* 405:5817–24
81. Herrera A, Fernández-Valle E, Martínez-Álvarez R, Molero D, Pardo ZD, et al. 2009. Real-time monitoring of organic reactions with two-dimensional ultrafast TOCSY NMR spectroscopy. *Angew. Chem.* 48:6274–77
82. Herrera A, Fernández-Valle E, Gutiérrez EM, Martínez-Álvarez R, Molero D, et al. 2010. 2D ultrafast HMBC: a valuable tool for monitoring organic reactions. *Org. Lett.* 12:144–47
83. Giraudeau P, Lemeunier P, Coutand M, Doux J-M, Gilbert A, et al. 2011. Ultrafast 2D NMR applied to the kinetic study of D-glucose mutarotation in aqueous solution. *J. Spectrosc. Dyn.* 1:2
84. Pardo ZD, Olsen GL, Fernández-Valle ME, Frydman L, Martínez-Álvarez R, Herrera A. 2012. Monitoring mechanistic details in the synthesis of pyrimidines via real-time, ultrafast multidimensional NMR spectroscopy. *J. Am. Chem. Soc.* 134:2706–15
85. Queiroz LHK Jr, Giraudeau P, dos Santos FAB, Oliveira KT, Ferreira AG. 2012. Real-time mechanistic monitoring of an acetal hydrolysis using ultrafast 2D NMR. *Magn. Reson. Chem.* 50:496–501
86. Corazza A, Rennella E, Schanda P, Mimmi MC, Cutuil T, et al. 2010. Native-unlike long-lived intermediates along the folding pathway of the amyloidogenic protein β_2-microglobulin revealed by real-time two-dimensional NMR. *J. Biol. Chem.* 285:5827–35
87. Gal M, Schanda P, Brutscher B, Frydman L. 2007. UltraSOFAST HMQC NMR and the repetitive acquisition of 2D protein spectra at Hz rates. *J. Am. Chem. Soc.* 129:1372–77
88. Lee M-K, Gal M, Frydman L, Varani G. 2010. Real-time multidimensional NMR follows RNA folding with second resolution. *Proc. Natl. Acad. Sci. USA* 107:9192–97
89. Kwakye JK. 1985. Use of NMR for quantitative analysis of pharmaceuticals. *Talanta* 32:1069–71
90. Holzgrabe U. 2010. Quantitative NMR spectroscopy in pharmaceutical applications. *Prog. Nucl. Magn. Reson. Spectrosc.* 57:229–40
91. Lindon JC, Nicholson JK, Holmes E, Everett JR. 2000. Metabonomics: metabolic processes studied by NMR spectroscopy of biofluids. *Concepts Magn. Reson.* 12:289–320
92. Wishart DS. 2008. Quantitative metabolomics using NMR. *TrAC Trends Anal. Chem.* 27:228–37
93. Zhang S, Nagana Gowda GA, Asiago V, Shanaiah N, Barbas C, Raftery D. 2008. Correlative and quantitative 1H NMR-based metabolomics reveals specific metabolic pathway disturbances in diabetic rats. *Anal. Biochem.* 383:76–84
94. Tenailleau E, Lancelin P, Robins RJ, Akoka S. 2004. Authentication of the origin of vanillin using quantitative natural abundance ^{13}C NMR. *J. Agric. Food Chem.* 52:7782–87
95. Le Grand F, George G, Akoka S. 2005. Natural abundance 2H-ERETIC-NMR authentication of the origin of methyl salicylate. *J. Agric. Food. Chem.* 53:5125–29
96. Kruger NJ, Troncoso-Ponce MA, Ratcliffe RG. 2008. 1H NMR metabolite fingerprinting and metabolomic analysis of perchloric acid extracts from plant tissues. *Nat. Protoc.* 3:1001–12
97. Le Gall G, Colquhoun IJ, Davis AL, Collins GJ, Verhoeyen ME. 2003. Metabolite profiling of tomato (*Lycopersicon esculentum*) using ^{1}H NMR spectroscopy as a tool to detect potential unintended effects following a genetic modification. *J. Agric. Food. Chem.* 51:2447–56
98. Weljie AM, Newton J, Mercier P, Carlson E, Slupsky CM. 2006. Targeted profiling: quantitative analysis of ^{1}H NMR metabolomics data. *Anal. Chem.* 78:4430–42
99. Giraudeau P, Guignard N, Hillion H, Baguet E, Akoka S. 2007. Optimization of homonuclear 2D NMR for fast quantitative analysis: application to tropine-nortropine mixtures. *J. Pharmaceut. Biomed. Anal.* 43:1243–48
100. Koskela H, Kilpeläinen I, Heikkinen S. 2005. Some aspects of quantitative 2D NMR. *J. Magn. Reson.* 174:237–44
101. Koskela H, Väänänen T. 2002. Quantitative determination of aliphatic hydrocarbon compounds by 2D NMR. *Magn. Reson. Chem.* 40:705–15
102. Lewis IA, Karsten RH, Norton ME, Tonelli M, Westler WM, Markley JL. 2010. NMR method for measuring carbon-13 isotopic enrichment of metabolites in complex solutions. *Anal. Chem.* 82:4558–63

103. Lewis IA, Schommer SC, Hodis B, Robb KA, Tonelli M, et al. 2007. Method for determining molar concentrations of metabolites in complex solutions from two-dimensional ^{1}H-^{13}C NMR spectra. *Anal. Chem.* 79:9385–90
104. Martineau E, Giraudeau P, Tea I, Akoka S. 2011. Fast and precise quantitative analysis of metabolic mixtures by 2D ^{1}H INADEQUATE NMR. *J. Pharm. Biomed. Anal.* 54:252–57
105. Martineau E, Tea I, Akoka S, Giraudeau P. 2012. Absolute quantification of metabolites in breast cancer cell extracts by quantitative 2D 1H INADEQUATE NMR. *NMR Biomed.* 25:985–92
106. Massou S, Nicolas C, Letisse F, Portais J-C. 2007. Application of 2D-TOCSY NMR to the measurement of specific ^{13}C-enrichments in complex mixtures of ^{13}C-labeled metabolites. *Metab. Eng.* 9:252–57
107. Zhang L, Gellerstedt G. 2007. Quantitative 2D HSQC NMR determination of polymer structures by selecting suitable internal standard references. *Magn. Reson. Chem.* 45:37–45
108. Giraudeau P, Akoka S. 2013. Fast and ultrafast quantitative 2D NMR: vital tools for efficient metabolomic approaches. *Adv. Bot. Res.* 67:99–158
109. Martineau E, Akoka S, Boisseau R, Delanoue B, Giraudeau P. 2013. Fast quantitative ^{1}H-^{13}C 2D NMR with very high precision. *Anal. Chem.* 85:4777–83
110. Gronwald W, Klein MS, Kaspar H, Fagerer SR, Nurnberger N, et al. 2008. Urinary metabolite quantification employing 2D NMR spectroscopy. *Anal. Chem.* 80:9288–97
111. Hu F, Furihata K, Kato Y, Tanokura M. 2007. Nondestructive quantification of organic compounds in whole milk without pretreatment by two-dimensional NMR spectroscopy. *J. Agric. Food Chem.* 55:4307–11
112. Giraudeau P, Remaud GS, Akoka S. 2009. Evaluation of ultrafast 2D NMR for quantitative analysis. *Anal. Chem.* 81:479–84
113. Pathan M, Akoka S, Tea I, Charrier B, Giraudeau P. 2011. "Multi-scan single shot" quantitative 2D NMR: a valuable alternative to fast conventional quantitative 2D NMR. *Analyst* 136:3157–63
114. Le Guennec A, Tea I, Antheaume I, Martineau E, Charrier B, et al. 2012. Fast determination of absolute metabolite concentrations by spatially-encoded 2D NMR: application to breast cancer cell extracts. *Anal. Chem.* 84:10831–37
115. Giraudeau P, Massou S, Robin Y, Cahoreau E, Portais J-C, Akoka S. 2011. Ultrafast quantitative 2D NMR: an efficient tool for the measurement of specific isotopic enrichments in complex biological mixtures. *Anal. Chem.* 83:3112–19
116. Pathan M, Akoka S, Giraudeau P. 2012. Ultrafast hetero-nuclear 2D J-resolved spectroscopy. *J. Magn. Reson.* 214:335–39
117. Cardoza LA, Almeida VK, Carr A, Larive CK, Graham DW. 2003. Separations coupled with NMR detection. *Trends Anal. Chem.* 22:766–75
118. Corcoran O, Spraul M. 2003. LC-NMR-MS in drug discovery. *Drug Discov. Today* 8:624–31
119. Exarchou V, Krucker M, van Beek TA, Vervoort J, Gerothanassis IP, Albert K. 2005. LC-NMR coupling technology: recent advancements and applications in natural products analysis. *Magn. Reson. Chem.* 43:681–87
120. Zhou Z, Lan W, Zhang W, Zhang X, Xia S, et al. 2007. Implementation of real-time two-dimensional nuclear magnetic resonance spectroscopy for on-flow high-performance liquid chromatography. *J. Chromatogr. A* 1154:464–68
121. Shapira B, Karton A, Aronzon D, Frydman L. 2004. Real-time 2D NMR identification of analytes undergoing continuous chromatographic separation. *J. Am. Chem. Soc.* 126:1262–65
122. Queiroz LHK Jr, Queiroz DPK, Dhooghe L, Ferreira AG, Giraudeau P. 2012. Real-time separation of natural products by ultrafast 2D NMR coupled to on-line HPLC. *Analyst* 137:2357–61
123. Adams RW, Aguilar JA, Atkinson KD, Cowley AJ, Elliott PIP, et al. 2009. Reversible interactions with para-hydrogen enhance NMR sensitivity by polarization transfer. *Science* 323:1708–11
124. Eisenschmid TC, Kirss RU, Deutsch PP, Hommeltoft SI, Eisenberg R, et al. 2002. Para hydrogen induced polarization in hydrogenation reactions. *J. Am. Chem. Soc.* 109:8089–91
125. Albert MS, Cates GD, Driehuys B, Happer W, Saam B, et al. 1994. Biological magnetic resonance imaging using laser-polarized ^{129}Xe. *Nature* 370:199–201
126. Navon G, Song Y-Q, Rõõm T, Appelt S, Taylor RE, Pines A. 1996. Enhancement of solution NMR and MRI with laser-polarized xenon. *Science* 271

127. Wolber J, Ellner F, Fridlund B, Gram A, Jóhanesson H, et al. 2004. Generating highly polarized nuclear spins in solution using dynamic nuclear polarization. *Nucl. Instrum. Methods Phys. Res. A* 526:173–81
128. Hausser KH, Stehlik D. 1968. Dynamic nuclear polarization in liquids. *Adv. Magn. Reson.* 3:79–139
129. Ardenkjaer-Larsen JH, Fridlund B, Gram A, Hansson G, Hansson L, et al. 2003. Increase in signal-to-noise ratio of >10,000 times in liquid state NMR. *Proc. Natl. Acad. Sci. USA* 100:10158–63
130. Joo C-G, Hu K-N, Bryant J-A, Griffin RG. 2006. In situ temperature jump high-frequency dynamic nuclear polarization experiments: enhanced sensitivity in liquid-state NMR spectroscopy. *J. Am. Chem. Soc.* 128:9428–32
131. Krahn A, Lottmann P, Marquardsen T, Tavernier A, Türke A-T, et al. 2010. Shuttle DNP spectrometer with a two-center magnet. *Phys. Chem. Chem. Phys.* 12:5830–40
132. Leggett J, Hunter R, Granwehr J, Panek R, Perez-Linde AJ, et al. 2010. A dedicated spectrometer for dissolution DNP NMR spectroscopy. *Phys. Chem. Chem. Phys.* 12:5883–92
133. Frydman L, Blazina D. 2007. Ultrafast two-dimensional nuclear magnetic resonance spectroscopy of hyperpolarized solutions. *Nat. Phys.* 3:415–19
134. Mishkovsky M, Frydman L. 2008. Progress in hyperpolarized ultrafast 2D NMR spectroscopy. *Chem. Phys. Chem.* 9:2340–48
135. Giraudeau P, Shrot Y, Frydman L. 2009. Multiple ultrafast, broadband 2D NMR spectra of hyperpolarized natural products. *J. Am. Chem. Soc.* 131:13902–3
136. Panek R, Granwehr J, Leggett J, Kockenberger W. 2010. Slice-selective single scan proton COSY with dynamic nuclear polarisation. *Phys. Chem. Chem. Phys.* 12:5771–78
137. Lloyd LS, Adams RW, Bernstein M, Coombes S, Duckett SB, et al. 2012. Utilization of SABRE-derived hyperpolarization to detect low-concentration analytes via 1D and 2D NMR methods. *J. Am. Chem. Soc.* 134:12904–07
138. Vold RL, Waugh JS, Klein MP, Phelps DE. 1968. Measurement of spin relaxation in complex systems. *J. Chem. Phys.* 48:3831–32
139. Bhattacharyya R, Kumar A. 2004. A fast method for the measurement of long spin-lattice relaxation times by single scan inversion recovery experiment. *Chem. Phys. Lett.* 383:99–103
140. Loening NM, Thrippleton MJ, Keeler J, Griffin RG. 2003. Single-scan longitudinal relaxation measurements in high-resolution NMR spectroscopy. *J. Magn. Reson.* 164:321–28
141. Smith PE, Donovan KJ, Szekely O, Baias M, Frydman L. 2013. Ultrafast NMR T1 relaxation measurements: probing molecular properties in real time. *Chem. Phys. Chem.* 14:3138–45
142. Barjat H, Morris GA, Smart S, Swanson AG, Williams SCR. 1995. High-resolution diffusion-ordered spectroscopy (HR-DOSY)—a new tool for the analysis of complex mixtures. *J. Magn. Reson. Ser. B* 108:170–72
143. Shrot Y, Frydman L. 2008. Single-scan 2D DOSY NMR spectroscopy. *J. Magn. Reson.* 195:226–31
144. Xu X, Lee J-S, Jerschow A. 2013. Ultrafast scanning of exchangeable sites by NMR spectroscopy. *Angew. Chem.* 52:8281–84
145. Wolff SD, Balaba RS. 1990. NMR imaging of labile proton exchange. *J. Magn. Reson.* 86:164–69
146. Shrot Y, Frydman L. 2003. Single-scan NMR spectroscopy at arbitrary dimensions. *J. Am. Chem. Soc.* 125:11385–96
147. Giraudeau P, Cahoreau E, Massou S, Pathan M, Portais J-C, Akoka S. 2012. UFJCOSY: a fast 3D NMR method for measuring isotopic enrichments in complex samples. *Chem. Phys. Chem.* 13:3098–101
148. Roussel T, Giraudeau P, Ratiney H, Akoka S, Cavassila S. 2012. 3D localized 2D ultrafast J-resolved magnetic resonance spectroscopy: in vitro study on a 7T imaging system. *J. Magn. Reson.* 215:50–65
149. Pelupessy P, Renella E, Bodenhausen G. 2009. High-resolution NMR in magnetic fields with unknown spatiotemporal variations. *Science* 324:1693–97
150. Zhang Z, Chen H, Wu C, Wu R, Cai S, Chen Z. 2013. Spatially encoded ultrafast high-resolution 2D homonuclear correlation spectroscopy in inhomogeneous fields. *J. Magn. Reson.* 227:39–45

Annual Review of
Analytical Chemistry

Volume 7, 2014

Contents